



저작자표시-비영리-변경금지 2.0 대한민국

이용자는 아래의 조건을 따르는 경우에 한하여 자유롭게

- 이 저작물을 복제, 배포, 전송, 전시, 공연 및 방송할 수 있습니다.

다음과 같은 조건을 따라야 합니다:



저작자표시. 귀하는 원저작자를 표시하여야 합니다.



비영리. 귀하는 이 저작물을 영리 목적으로 이용할 수 없습니다.



변경금지. 귀하는 이 저작물을 개작, 변형 또는 가공할 수 없습니다.

- 귀하는, 이 저작물의 재이용이나 배포의 경우, 이 저작물에 적용된 이용허락조건을 명확하게 나타내어야 합니다.
- 저작권자로부터 별도의 허가를 받으면 이러한 조건들은 적용되지 않습니다.

저작권법에 따른 이용자의 권리는 위의 내용에 의하여 영향을 받지 않습니다.

이것은 [이용허락규약\(Legal Code\)](#)을 이해하기 쉽게 요약한 것입니다.

[Disclaimer](#)

Master's Thesis of Science of Agriculture

**Proteomic and Transcriptomic Identification
of Host Factors Associated with Susceptibility
to Cucumber Mosaic Virus**

단백체 및 전사체 분석을 통한
오이모자이크 바이러스 감수성 관련 기주 인자 구명

August 2019

Soo-Jung Han

**Department of International Agriculture Technology
Graduate School of International Agriculture Technology
Seoul National University**

ABSTRACT

Proteomic and Transcriptomic Identification of Host Factors Associated with Susceptibility to Cucumber Mosaic Virus

Soo-Jung Han

**Major of International Agricultural Technology
Department of International Agricultural Technology
Graduate School of International Agricultural Technology
Seoul National University**

Plant viruses are important pathogens that cause severe crop losses. The most efficient method to control viral diseases is currently to use virus resistant crops. In order to develop virus resistant crops, a detailed understanding of the molecular interactions between viral and host proteins is necessary. Recessive resistance to a pathogen can be conferred when plant genes essential in the life cycle of a pathogen are deficient. In this study, we aimed to identify and characterize host factors associated with cucumber mosaic virus (CMV) that causes severe damages in various crops. We utilized proteomic and transcriptomic approaches to identify the host factors. In the proteomic approach, three CMV proteins, 1a, 2a, and MP, were fused with the FLAG or HA tag and expressed in plant cells using CMV infectious cDNA constructs. Among the FLAG-tagged and HA-tagged constructs, the recombinant CMV clones carrying a FLAG-tag at the N-terminus of 2a and a HA-tag at the C-

terminus of 1a were competent for replication. To identify 2a-interacting host proteins, *Nicotiana benthamiana* plants were inoculated with the recombinant CMV expressing the FLAG-tagged 2a. Crude extracts obtained from the systemically infected leaves were immunoprecipitated using anti-FLAG antibodies. The resulting product was subjected to sodium dodecyl sulfate-polyacrylamide gel electrophoresis (SDS-PAGE) followed by liquid chromatography technique coupled with tandem mass spectrometry (LC-MS/MS) analysis. This approach identified several putative 2a-interacting host proteins, including glyceraldehyde 3-phosphate dehydrogenase-A (GAPDH-A) and eukaryotic translation initiation factor 4A (eIF4A). To identify host genes associated with susceptibility to CMV, transcriptomic reprogramming upon CMV infection was analyzed by RNA sequencing. Comparative analysis of differentially expressed genes (DEGs) showed that various stress-related and hormone-related genes were transcriptionally regulated by CMV infection. Especially, DEGs related to ethylene biosynthesis and signaling were positively regulated. Indeed, ethylene production was increased upon CMV infection. Exogenous ethylene treatments of peppers infected with CMV resulted in increase of symptom severity and viral accumulation. In addition, RNA sequencing revealed that CMV infection caused down-regulation of cell cycle-associated genes, suggesting that cell division might be suppressed in the CMV-infected tissues. Therefore, we suggest that modulating hormone-related and cell cycle-related host genes by CMV infection might be correlated with the CMV-induced symptoms, such as mosaic, chlorosis, and stunting. Our approaches can provide new insights into understanding molecular interactions between host and viruses and underlying mechanisms of physiological changes upon viral infections.

.....
Keyword: Recessive resistance, Host–virus interaction, Cucumber mosaic virus, Host factors, Susceptibility genes

Student Number: 2017-27078

CONTENTS

| | |
|--|------------|
| Abstract | i |
| Contents | iv |
| List of Figures | vi |
| List of Tables | vii |
| Introduction | 1 |
| Materials and Methods | 5 |
| 1. Plant growth and inoculation | 5 |
| 2. Tagging CMV genes by engineering infectious cDNA clones | 5 |
| 3. RNA extraction and RT-PCR | 6 |
| 4. SDS-PAGE and Western blot | 7 |
| 5. Immunoprecipitation and LC-MS/MS analysis | 7 |
| 6. Subcellular localization | 8 |
| 7. RNA sequencing | 9 |
| 8. Analysis of differentially expressed genes (DEGs) | 9 |
| 9. Gene ontology (GO) functional enrichment analysis | 10 |
| 10. KEGG Pathway enrichment analysis | 10 |
| 11. Ethylene measurement | 10 |
| 12. Exogenous ethylene treatment to peppers | 11 |

| | |
|--|-----------|
| Results | 12 |
| 1. pCMV-FLAG:2a cDNA infectious clone is competent for CMV replication | 12 |
| 2. Subcellular localization of CMV 1a and 2a in <i>N. benthamiana</i> leaf cells | 15 |
| 3. Candidate host factors interacting with CMV viral protein 2a were found by using Co-IP and LC-MS/MS | 18 |
| 4. Analysis of Differentially expressed genes (DEGs) in response to CMV and/or BBWV2 infection | 20 |
| 5. Gene ontology (GO) terms and enrichment analysis of identified DEGs upon CMV | 31 |
| 6. Important KEGG pathways influenced by CMV infection | 39 |
| 7. Ethylene production by pepper leaves following CMV infection | 45 |
| 8. Exogenous ethylene treatment to CMV infected peppers affects symptom development and viral accumulation | 45 |
| Discussion | 49 |
| References | 55 |
| Abstract in Korean | 63 |

LIST OF FIGURES

| | |
|--|----|
| Figure 1. Diagram of FLAG or HA-tagged CMV infectious clones and infectivity test results in <i>N. benthamiana</i> | 13 |
| Figure 2. FLAG-tagging at the N-terminus of 2a (pCMV-FLAG:2a) is competent for CMV replication | 14 |
| Figure 3. Visualization of subcellular localization of CMV 1a and 2a | 16 |
| Figure 4. Screening for host factors interacting with CMV 2a protein using Co-IP and LC-MS/MS | 19 |
| Figure 5. Comparison of Symptoms of CMV, BBWV2 and CMV+BBWV2 | 22 |
| Figure 6. Comparison of differentially expressed genes (DEGs) in response to infection with CMV or/and BBWV2 | 25 |
| Figure 7. Gene Ontology (GO) terms analysis in CMV infection | 32 |
| Figure 8. GO enrichment analysis of up-regulated DEGs | 33 |
| Figure 9. GO enrichment analysis of down-regulated DEGs | 36 |
| Figure 10. Regulation of the genes associated with Cell cycle regulation upon CMV infection in pepper | 38 |
| Figure 11. Regulation of the genes associated with ethylene biosynthesis upon CMV infection in pepper. | 43 |
| Figure 12. Ethylene production by detached leaves of peppers infected with CMV, BBWV2 and CMV+BBWV2 | 46 |
| Figure 13. Effect of exogenous ethylene on the symptom development and viral accumulation | 47 |

LIST OF TABLES

| | |
|---|----|
| Table 1. Symptoms induced by CMV, BBWV2 and CMV+BBWV2 in pepper cv. ‘Shinhong’ | 23 |
| Table 2. Read statistics for RNA Sequencing of pepper plants in response to infection with CMV, BBWV2 and CMV+BBWV2 | 24 |
| Table 3. Top 20 up and down DEGs in response to infection with CMV ... | 28 |
| Table 4. Top 20 up and down DEGs in response to infection with BBWV2 | 29 |
| Table 5. Top 20 up and down DEGs in response to infection with CMV+BBWV2 | 30 |
| Table 6. KEGG pathway enrichment analysis upon CMV infection by DAVID 6.8. | 40 |
| Table 7. DEGs related to Hormone synthesis and signaling in response to infection with CMV | 41 |

INTRODUCTION

Susceptible plants to viruses must provide a proper environment for the viral life cycle. Plant viruses should be able to replicate in infected cells, move from cell to cell through plasmodesmata, and induce systemic infection through vascular tissues (Truniger & Aranda, 2009). Their coding capacity is limited and they must rely on various host factors for every stage in their infection cycle (Nagy & Pogany, 2011). Therefore, identifying host factors which interact with viral proteins is important to develop new methods to control viral diseases and to understand virus life cycles.

One of the most important constraints limiting crop production is viral disease. Conventional ways to control viral diseases were focused on vector management using pesticides, natural predators, or physical materials like mulches without considering epidemiological factors related to virus disease outbreaks (Legg et al., 2014). Frequent mutations due to error-prone viral replications make virus to avoid plant defense systems and make it difficult to develop long-term disease management strategies (Loebenstein & Katis, 2014). The most effective and environmentally sensitive approach to the disease control is utilizing genetic resistance in plants by enhancing the plant immunity (Zaidi et al., 2016).

There are two ways to achieve plant host resistance to virus. The one is using dominant resistance (*R*) genes and the other one is related to recessive resistance genes (Hashimoto et al., 2016). *R* gene-mediated dominant resistance is usually activated by specific viral proteins, termed avirulence factors (*Avr*). *R* gene products have conserved nucleotide-binding (NB) and a C-terminal leucine-rich repeat (LRR) domains and recognize the presence of a specific pathogen directly or indirectly (Moffett, 2009). Screening for natural sources of resistance to viruses and molecular characterization of the identified

dominant *R* genes revealed that most of the known antiviral R proteins are NB-LRRs (Wang, 2018). Plant breeders have been using the genes (*R* genes) to control diseases in plants (DAC & P, 2002). However, mutations of viral effector proteins may lead to the occurrence of resistance breaking isolates factors (Wang, 2018). Recessive resistance to viruses can be conferred when plant genes essential in the life cycle of pathogens are deficient. The absence of appropriate host factors or inhibition of the interactions between viral proteins and corresponding host factors may lead recessive resistance (Truniger & Aranda, 2009). Recessive resistance usually works more stably and broadly than dominant resistance. The majority of the recessive resistance genes known against plant viruses have been reported for potyviruses (Kang et al., 2005) and encode translation initiation factors of the 4E or 4G family (eIF4E/eIF4G) (Robaglia & Caranta, 2006). Mutations in eIF4Es confer loss-of-susceptibility to potyviruses and several viruses (Mazier et al., 2011). To enable developing recessive resistance crop against a wide range of plant viruses, it is important to improve the genetic resources available for recessive resistance other than eIF4Es (Hashimoto et al., 2016).

Cucumber mosaic virus (CMV), a member of the genus *Cucumovirus* in the family *Bromoviridae*, is the greatest constraint especially to pepper production in Korea for decades. CMV has a tripartite, positive sense RNA genome of three RNAs designated as RNA 1, 2 and 3. RNA 1 encodes 1a protein (110 kDa) with methyltransferase domain for RNA capping in the N-terminal half and a helicase-like domain in the C-terminal half. RNA2 encodes 2a protein (97 kDa) which has a core RNA-dependent RNA polymerase (RdRp) domain required for RNA synthesis (Palukaitis & Garcia-Arenal, 2003). Physical interaction between 1a and 2a is important for the formation of functional replicase complex that is associated with the vacuolar membrane, tonoplast (Cillo et al., 2002). RNA 3 encodes 3a (MP) and CP proteins related to the virus movement.

Plant viruses including CMV require various host factors to complete the steps of their life cycle. The investigation for host factors involved in virus replication has been one of the main subject of virus research and addressed through different approaches including in reverse and forward genetics and intracellular localization studies (Carbonell et al., 2016). Recent advances in proteomic analysis and genome-wide screenings in the model organism have been extremely useful in identifying novel host factors participating in the virus replication (Galao et al., 2007; Nagy et al., 2014). Generally, host factors control the biogenesis of replication organelles, the composition, assembly or activity of the viral replication complexes (VRCs), or mediate post-translational modifications of viral replication proteins (Carbonell et al., 2016). However, only a small amount of host factors associated with CMV replication complex have been identified. Identified host factors in CMV include proteins involved in association of VRC to the tonoplast (TIP1, TIP2) and phosphorylation of viral RNA polymerase to inhibit replication (CIPK12) (Kim et al., 2006; Kim et al., 2002).

Investigating host genes which is related to distinct virus symptom expression can be the way of understanding host-virus interactions. In many cases, each virus can induce specific symptoms in a host plant and the same virus can induce different symptoms in different host plants (Whitham et al., 2003). Interacting between viral components and host factors would cause an alteration in the plant physiology resulting in the development of symptoms (Pallas & Antonio, 2011). Indeed, recent discoveries have evidenced that plant development is affected by plant–virus interactions, which interfere with a broad range of cellular processes, such as hormonal regulation, cell cycle control and endogenous transport of macromolecules (Culver & Padmanabhan, 2007; Kong et al., 2000). Thus, analysis of the differential regulation of genes involved in symptom development and identification of the critical regulatory components with transcriptome analysis can provide molecular understanding

of disease symptoms and new insights into reducing the severity of symptoms (Seo et al., 2018).

Pepper (*Capsicum annuum*) is an economically important vegetable worldwide. In Korea, Cucumber mosaic virus (CMV) and Broad bean wilt virus (BBWV2) are two major viruses limiting pepper production (Kwon et al., 2018). The symptoms of CMV infection in pepper include mosaic, size reduction, distortion of the leaves and stunting (Gallitelli, 2000). CMV can sometimes cause severe infections in synergy with other viruses such as BBWV2 in pepper plants (Kwon et al., 2018). Broad bean wilt virus 2 (BBWV2), a member of the genus Fabavirus in the family Secoviridae, is a widespread viral pathogen that infects many economically important crops, including pepper, spinach, and sesame. The BBWV2 genome is composed of two single-stranded positive-sense RNA molecules, RNA1 and RNA2, which are encapsulated separately into icosahedral virions (Ferrer et al., 2011). BBWV2 RNA1 and RNA2, which are approximately 5960 and 3600 nucleotides in length, respectively, encode single large open reading frames (ORFs). BBWV2 causes various symptoms, including vein chlorosis, leaf malformation, yellowing in pepper.

In this study, we tried to identify the host genes which are highly related to CMV susceptibility to understand the molecular interactions between viral and host proteins. Using proteomic approach, host factors interacting CMV viral protein 2a were identified by co-immunoprecipitation in *N.benthamiana*. We also figured out host genes which were highly regulated during CMV infection through RNA sequencing data to understand the molecular mechanisms related to the distinct symptoms induced by CMV in pepper.

MATERIALS AND METHODS

1. Plant growth and inoculation.

N.benthamiana and pepper plants were grown in a growth chamber at 24 °C/18°C (16h light /8h dark). Plasmid DNAs for Agro-transformation were prepared using the Plasmid Miniprep Kit (QIAGEN, USA). *Agrobacterium tumefaciens* strain EHA105 and GV3101 were transformed with approximately 2ug of plasmid DNA. In case of pCMV-R1-1a-FLAG and of pCMV-R1-FLAG-1a Clones, EHA105 strain was transformed by electroporation (Bio-Rad, USA). Clones were selected on Kanamycin (100ug/ul) and Rifampicin (50ug/ul) plates. For CMV-R1 clones, Kanamycin (50ug/ul) and Rifampicin (50ug/ul) plates were used. All CMV cDNA infectious clones used in this study were agro-infiltrated ($OD_{600} = 0.7$). These were inoculated to 5ml LB broth with appropriate antibiotics and incubated in shaking incubator at 220rpm at 28°C for overnight. After transferring to fresh LB media with appropriate antibiotics and 20uM Acetosyringone, the subculture media was incubated in shaking incubator at 220rpm at 28°C for 12 hours. with LB broth (appropriate antibiotics, 20uM Acetosyringone). The culture was resuspended to $OD_{600} = 0.7$ with infiltration buffer (10mM MES, 10mM MgCl₂ and 200uM Acetosyringone, pH 5.6). Resuspended cultures were incubated in shaking incubator at 220rpm at 28°C for 4hours. Cultures were mixed together in equal proportions and infiltrated onto the abaxial surface of 3 weeks old *N.benthamiana* leaves using 1 ml syringe.

2. Tagging CMV genes by engineering infectious cDNA clones

Recognition sites of restriction enzymes were introduced into the 5' and 3' ends of the synthetic genes for partial 1a:FLAG, FLAG:1a and FLAG:2a; BamHI and Kpn I to 1a:FLAG, EcoR I and Xba I to FLAG:1a , Xba I sites to FLAG:2a. The synthetic genes were removed from pBHA vector by enzyme

digestion and inserted into the pSNU-based CMV CDNA infectious clones (pCMV-R1, pCMV-R2). FLAG sequence was added to MP by PCR with three primers for MP:FLAG (5'-ATGGCTTTCCAAGGTACCAGTA-3', 5'-CATCGTCGTCCTTGTAGTCAAGACCGTTAACCACCTGC-3', 5'-ATCGACGCGTCTTGTGCATCGTCGTCCTTGTAGTCAA-3') and for FLAG:MP (5'-TCATCGTCGTCCTTGTAGTCAGCCATGCCTCGGGAA ATC -3', 5'-GAAAGCCTTGTGCATCGTCGTCCTTGTAGTC-3', 5'-GGACGACGATGACAAGGCTTTCCAAGGTACCAGTAG-3', 5'-ATCGACGCGTAAGACCGTTAACCACCTGCG-3'). MP:FLAG and FLAG:MP region spanning from the Kpn I site to the 3' end of Mlu I was cloned into pCMV-R3-dMP plasmid which was opened with the Kpn I and Mlu I enzyme sites. pCMV-R1-1a:HA was constructed with three primers by PCR with three primers (5'-GATGTTCCAGATTACGCTTAGCGGTCTCCCTCTTCGG -3', 5'-TGGAACATCGTATGGGTAAGCACGAGCAACACATTCG -3', 5'-GACCGCTAAGCGTAATCTGGAACATCGTATGGGTAAG -3').

3. RNA extraction and RT-PCR

Total RNA was isolated from inoculated plants by using the PureLink[®] RNA Mini Kit (Ambion, USA) and analyzed by RT-PCR using the primer pairs. Total RNA was denatured at 65°C for 5 min with 10 µM of reverse primer. The RT reaction was incubated at 42°C for 1 h with reverse transcriptase M-MuLV (NEB, USA). To detect virus accumulation in the inoculated and upper uninoculated leaves, reverse primer (5'-ATGGTCTTCCGCCGATAACTC-3') was used to make the cDNA. The cDNA was amplified by 35 cycles of PCR using OneTaq DNA Polymerase (NEB, USA) with CMV-specific primers (5'-GATCCATTGCGCGAGGTTCA-3' and 5'-ATGGTCTTCCGCCGATAACTC -3'). For MP:HA and 1a:HA clones, RT primer(5'-AAGTACACGGACCGAAGT -3') and PCR primers(5'-GTCCAACCTATTAACCACCCA -3' and 5'-AGTCCTTCCGAAGAAACCTA -3') were used.

To evaluate the stability of the FLAG insertion of 2a in the progeny viruses,

we used (5'-GCTCTAGACAAATTAACGGAATCACC) primer for RT reaction. The cDNA was amplified by 35 cycles of PCR using Q5 DNA Polymerase (NEB, USA) and 10 µM of primers (5'- GCTCTAGAGGTTTAT TTACAAGAGCG-3' and 5'- GCTCTAGACAAATTAACGGAATCACC-3'). After initial denaturation at 94°C for 3 min, each cycle consisted of 30 s at 94°C, 30 s at 58°C, and 40 s at 68°C. PCR products were analyzed by agarose gel electrophoresis and sequenced.

4. SDS-PAGE and Western blot

Western blot was conducted to confirm whether FLAG:2a proteins were expressed in *N.benthamiana*. Total protein extraction from *N.benthamiana* leaves was performed using the TRIzol™ Reagent methods (Invitrogen, USA) according to the manufacturer's instructions. Total proteins for each sample were separated by 10% SDS-PAGE and transferred onto PVDF membrane. Proteins were probe with anti-FLAG antibody (1:1000) (Clontech, Japan), and anti-mouse antibody (1:5000) was used as secondary antibody. Immunoreactions were detected using the ECL-based system (Sigma-Aldrich, USA).

5. Immunoprecipitation and LC-MS/MS analysis

Total protein extracts were prepared from the infected leaves of *N.benthamiana* plants inoculated with pCMV-R2-FLAG:2a. At 10 dpi, the leaves were homogenized in three volumes of protein extraction buffer (1M Tris-HCl at pH 7.5, 5M NaCl, 1M MgCl₂, 1M DTT, 1% CHAPS, proteinase inhibitor cocktail (Sigma, USA). Cell debris was removed by centrifugation at 13,500 rpm for 10 min at 4 °C using cell strainers. The resulting supernatants were incubated with anti-FLAG antibody conjugated magnetic beads (ThermoFisher, USA) for overnight at 4 °C. The immunocomplexes were then precipitated by centrifugation for 10 min at 12,000 rpm and washed five times in 1 mL of the protein extraction buffer. The resulting samples were analyzed

by 12% SDS-PAGE and stained with Coomassie blue. The Xpert prestained protein marker (GenDEPOT, USA) was used as the ladder. After staining, bands of interest were excised from the gel and analyzed by LC-MS/MS. The LC-MS/MS analysis was performed at Yonsei Proteome Research Center (Seoul, South Korea). To identify and quantify peptides, LC was performed with an Easy n-LC 1000 system (Thermo Fisher Scientific, Rockford, IL, USA). A C18-nanobore column (150 mm × 0.1 mm, 3- μ m pore size, Agilent) was used for peptide separation. LTQ-Orbitrap mass spectrometry (Thermo Fisher, USA) was used to identify and quantify peptides. Xcalibur (version 2.1, Thermo Fisher Scientific, USA) was used to generate peak lists. The peak lists were examined by searching the National Center for Biotechnology Information database using the MASCOT search engine (<http://www.matrixscience.com>, Matrix Science, Boston, MA, USA). The acquired data were compared to the whole database with search parameters set as follows: enzyme, trypsin; allowance of up to one missed cleavage peptide; mass tolerance \pm 0.5 Da and MS/MS tolerance \pm 0.5 Da; modifications of methionine oxidation and cysteine carbamidomethylation when appropriate, with auto hits allowed and only significant hits to be reported. The proteins were identified on the basis of two or more peptides whose ion scores exceeded the threshold, $P < 0.05$, which indicated the 95% confidence level for these matched peptides.

6. Subcellular localization

To insert the fluorescence proteins, we made SalI and MfeI enzyme sites respectively on pCMV-R1-1a and pCMV-R2-2a constructs by fusion-PCR-based method using overlapping primers for each junction. RFP and GFP were amplified using Q5 DNA Polymerase (NEB, USA). RFP was cloned into pCMV-R1-1a which was opened with SalI site and GFP was inserted into pCMV-R2-2a which was opened with the MfeI enzyme site. The plasmids of these constructs were transformed into *Agrobacterium tumefaciens* strain EHA105 and mixed in equal proportions with *A. tumefaciens* cells harboring

pCMV-R1, pCMV-R2 and Vac-YFP constructs. Each mixture was infiltrated into the abaxial surface of the leaves of *N. benthamiana*. These vectors were transiently co-expressed in inoculated plants grown in a growth chamber at 24 °C/18°C (16h light /8h dark). The fluorescence of RFP and GFP signals at 7dpi were observed by Confocal fluorescence microscope (Leica, Germany) equipped with a specific laser/filter combination to detect CFP (excitation at 458 nm), GFP (excitation at 488 nm), and YFP (excitation at 514 nm).

7. RNA sequencing

After sap-inoculation, symptomatic upper pepper leaf samples at 7dpi were collected from the same nodes of ‘shinhong’ pepper plants infected with CMV, BBWV2 or CMV+BBWV2, respectively. Samples are frozen immediately in liquid nitrogen before use. Leaf samples from five peppers infected with each virus were pooled together for RNA isolation, thereby three RNA samples were obtained for CMV, BBWV2 or CMV+BBWV2 infected samples. Similarly, leaves from uninoculated plants were used as healthy controls. Total RNA was extracted using PureLink[®] RNA Mini Kit (Ambion, USA) and subjected to library construction. A total of twelve libraries was constructed and sequenced by an Illumina HiSeq. 2500 sequencer (Illumina, Inc., USA).

8. Analysis of differentially expressed genes (DEGs)

In order to compare the expression abundance among Healthy, CMV, BBWV2 and CMV+BBWV2 infected samples, Raw sequence reads were filtered by the Illumina pipeline and were mapped using the RNA-seq mapping algorithm in TopHat (v2.1.1) to the reference transcripts of *Capsicum annuum* (Annum.v.1.5.PEP.fa). The number of mapped clean reads for each gene was counted and then normalized with the DESeq package in R. Genes with significantly different expression were determined by log₂fold change ≥ 1

(for up-regulated transcripts), ≤ -1 (for down-regulated transcripts) with p-value cutoff of ≤ 0.05 . The regulation for each transcript was assigned based on log2fold change. Correlation analysis and hierarchical clustering were performed to group the genes according to patterns of expression using the gplot in R.

9. Gene ontology(GO) functional enrichment analysis

GO analysis was performed based on the protein sequence similarity in the GO database. The number of genes assigned in each GO term was counted using in-house scripts of SEEDERS Inc. (Daejeon, South Korea). The GO-terms with p-value less than or equal to 0.05 were considered as the significant enrichment. The biological process of enriched GO terms was visualized by using web-based program ReviGO (Supek et al., 2011). The data was plotted by using R program. We also used AgriGO (<http://bioinfo.cau.edu.cn/agriGO/analysis.php>), a web based tool for enrichment analysis.

10. KEGG Pathway enrichment analysis

Pathway enrichment analysis was based on the KEGG (Kyoto Encyclopedia of Genes and Genomes) database. Database for Annotation, Visualization, and Integrated Discovery (DAVID) v.6.8 (<https://david.ncifcrf.gov/tools.jsp>) was used to annotate input genes and classify gene functions (Huang da et al., 2009).

11. Ethylene measurement

Ethylene production from the virus-infected and healthy plants was measured at 10 dpi. Four grams of the symptomatic upper leaves were detached from the infected plants and enclosed in 100 ml plastic containers with a gas-sampling port. The containers were left at 26 °C in the dark. At 2h after the start of incubation, a 1 ml headspace air sample was taken and assayed for ethylene by a gas chromatograph equipped with a hydrogen flame ionization detector and

an alumina column. Ethylene production rates were measured with three air samples taken from a container and the mean value was obtained.

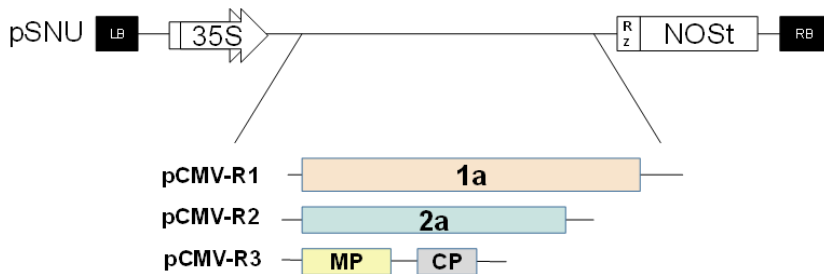
12. Exogenous ethylene treatment to peppers

CMV infected tobacco leaves were used as inoculum sources and ground in 50 mM sodium phosphate buffer (pH 7.5). Two-week old pepper seedlings were dusted with carborundum and then the ground inoculum was placed on the leaf and gently rubbed. Inoculated leaves were rinsed with tap water and incubated in a growth chamber. Healthy seedlings and seedlings inoculated with CMV at 4 dpi were exposed with different volumes (0ml, 0.5ml, 1ml, 2.5ml) of 10mM Ethephon (Sigma Aldrich, USA) for 3 days in 117000cm³ (65 x 45 x 40 cm) boxes at growth chamber. After 3 days, the leaves were collected and used for western blot and SDS-PAGE. Total protein extraction was performed by using the TRIzol™ Reagent methods (Invitrogen, USA) according to the manufacturer's instructions. Each sample was separated by 12% SDS-PAGE and transferred onto PVDF membrane. Proteins were probe with CMV anti-CP antibody (1:10000) (Seo et al., 2009) and anti-rabbit HRP linked antibody (1:5000) (Cell Signaling, USA) was used as secondary antibody. Immunoreactions were detected using the ECL-based system (Sigma-Aldrich, USA).

RESULTS

1. pCMV-FLAG:2a cDNA infectious clone is competent for CMV replication

To identify the host factors which interacts with CMV viral proteins including 1a, 2a and MP, we constructed recombinant CMV constructs tagged with FLAG or HA (Figure. 1). These constructs were verified by visual observation of symptoms and confirmed by RT-PCR with CMV specific primers. In case of pCMV-1a and pCMV-MP, they did not have infectivity when they were fused with FLAG tags (Figure. 1). FLAG:2a and 1a:HA have systemic infectivity on *N.benthamiana*. The infectivity of *N.benthamiana* inoculated by pCMV-FLAG:2a was confirmed by distinct CMV symptoms such as mosaic, yellowing and stunting in 30 plants (Figure. 2A). RT-PCR with CMV specific primers was conducted to detect the viral RNAs (Figure. 2B). Total RNA was extracted from *N. benthamiana* samples infected by CMV (wild type) and CMV (pCMV-FLAG:2a) at 7dpi. Healthy (non-inoculated) plants were used as a negative control. Expression of the FLAG-tagged 2a (98kDa) was confirmed by western blot analysis in extracts of infected *N. benthamiana* using anti-FLAG monoclonal antibody (Figure. 2C). In addition, we tested the stability of FLAG sequence insertion in the CMV 2a genome by transferring three times from plant to plant by mechanical sap-inoculation. The FLAG insertion in the 2a protein was not stably maintained during virus replication.



| Test Clone | Systemic Infection ^a (% infected plants) |
|----------------------|--|
| <i>N.benthamiana</i> | |
| pCMV-1a:FLAG | 0/32 (0) |
| pCMV-FLAG:1a | 0/10 (0) |
| pCMV-FLAG:2a | 30/30 (100) |
| pCMV-FLAG:MP | 0/25 (0) |
| pCMV-MP:FLAG | 0/18 (0) |
| pCMV-1a:HA | 12/12 (100) |

^a Number of infected plants/number of inoculated plants

Figure. 1. Diagram of FLAG or HA-tagged CMV infectious clones and infectivity test results in *N. benthamiana*. Construction of FLAG-tagged CMV infectious clones. RNA1, RNA2 and RNA3 of CMV cDNA infectious clones were modified by addition of FLAG or HA sequences at the N and/or C terminus of the 1a, 2a and MP proteins. Among the constructs, pCMV-FLAG:2a and pCMV-1a:HA have viral infectivity. Verified by visual observation of symptoms and confirmed by RT-PCR with CMV specific primers.

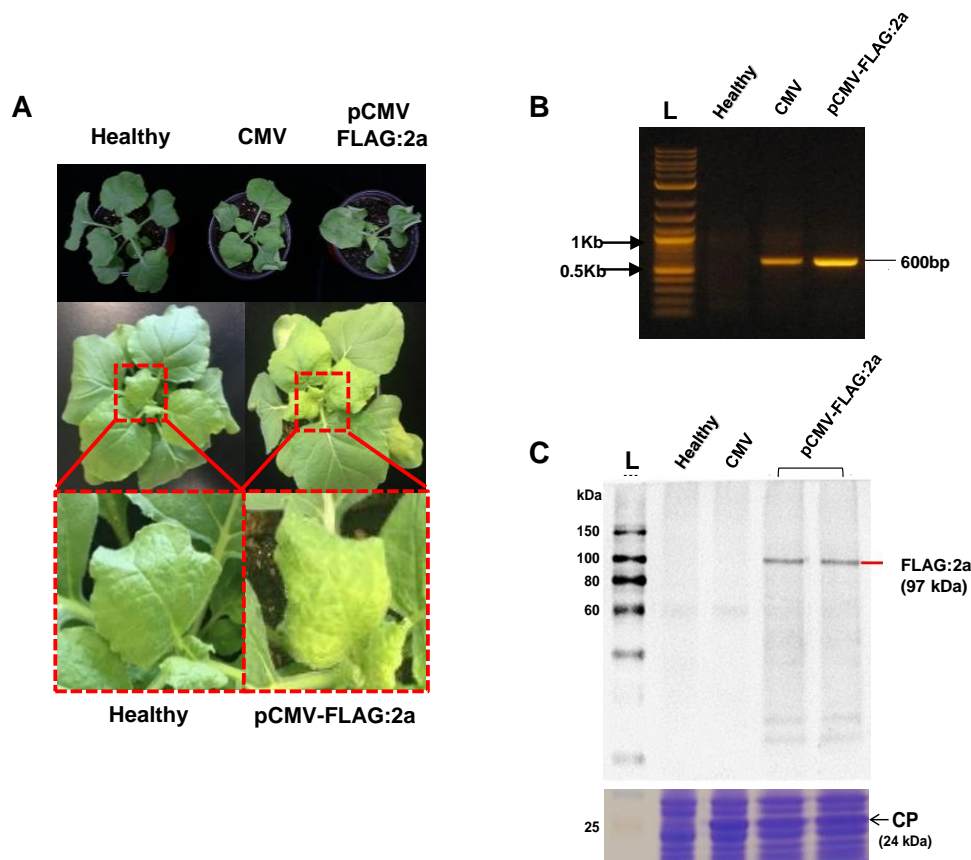


Figure 2. Flag-tagging at the N-terminus of 2a (pCMV-FLAG:2a) is competent for CMV replication. (A) Symptoms of pCMV-FLAG:2a infection in *Nicotiana benthamiana* (*N. benthamiana*). Infected plants show mosaic, stunting and leaf size reduction at 7dpi after Agro infiltration ($OD_{600}=0.7$). (B) Detection of CMV by RT-PCR with specific primers. Total RNA was extracted from *N. benthamiana* samples infected by CMV (Wild type) and CMV (pCMV-FLAG:2a). Healthy plants were used as a negative control. (C) Detection of FLAG:2a protein in vivo. Expression of the FLAG-tagged 2a was confirmed by Western blot analysis in extracts of infected *N. benthamiana* using anti-FLAG monoclonal antibody.

2. Subcellular localization of CMV 1a and 2a in *N. benthamiana* leaf cells.

To predict the location of host factors interacting with CMV replicase proteins, we needed to observe the subcellular localization of 1a and 2a proteins by using pCMV-1a:RFP and pCMV-GFP:2a constructs (Figure. 3). Upon translation of the viral genome, the viral membrane proteins target specific cytoplasmic organelles for the formation of the membrane-anchored viral replicase complexes (VRCs). Dependent on the type of virus, the sources of membranes may derive from different organelles such as the endoplasmic reticulum (ER), endosomes, mitochondria, peroxisomes and chloroplasts (Wang, 2015). In CMV replication, it is well known that CMV 1a and 2a proteins co-localized predominantly to the tonoplasts (Cillo et al., 2002)

The data showed that 1a:RFP was localized in vacuolar membranes (tonoplasts) with vesicle-like structures and GFP:2a was detected not only in tonoplasts but also in cytoplasm. (Figure. 3). There is a similar report in tobacco and cucumber plants that 2a was detected in the cytoplasm by western blotting of fractionated extracts from CMV-infected tissue. However, 2a was not observed in the cytoplasm by in situ hybridization. (Cillo et al., 2002). We suggest that CMV 1a might have an ability to recruit 2a proteins to the tonoplasts from cytoplasm and other host factors like BMV 1a proteins.

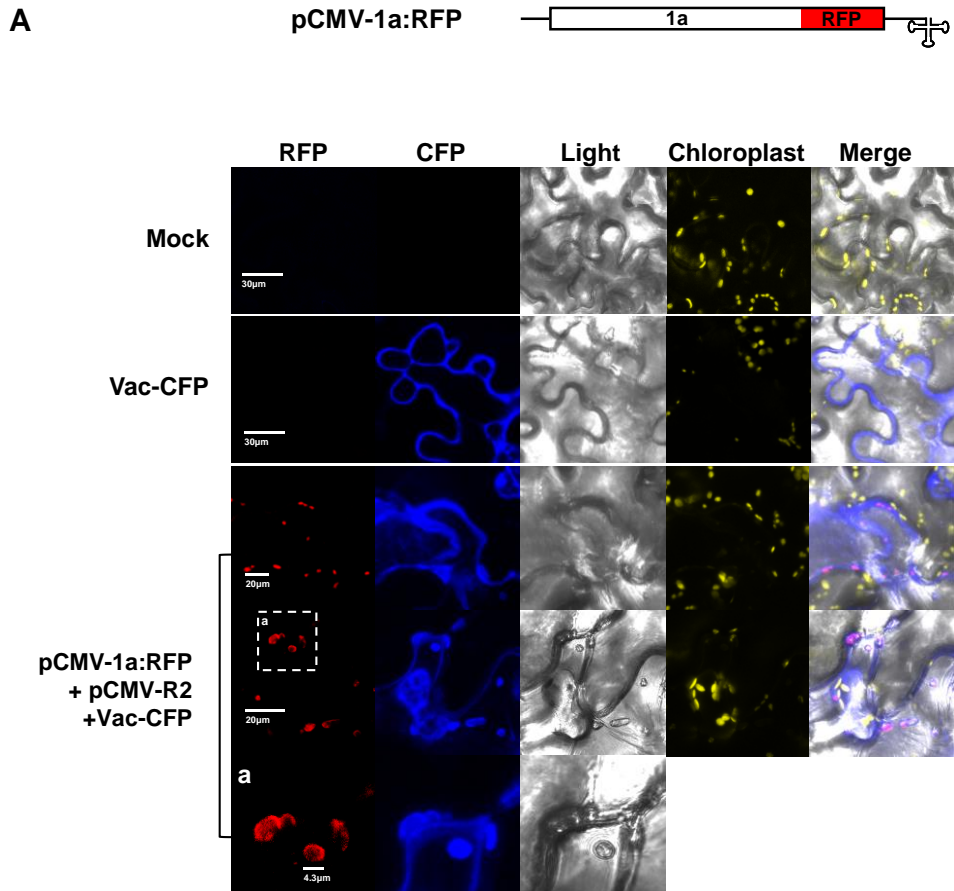
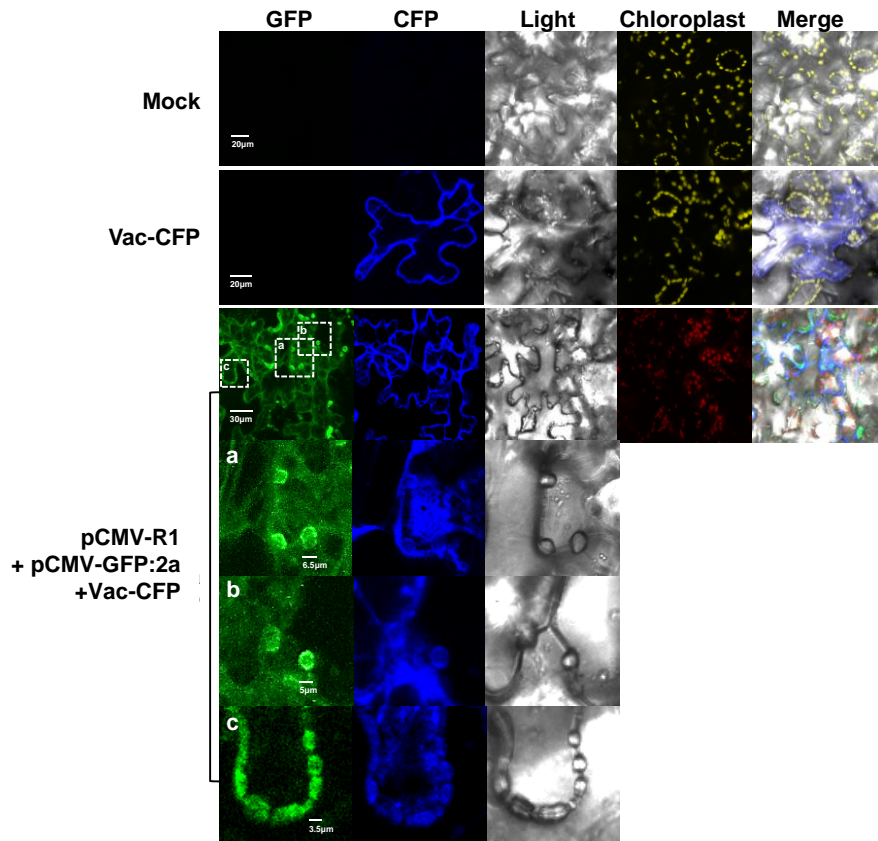
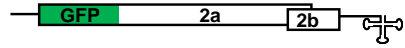


Figure. 3. Visualization of subcellular localization of CMV 1a and 2a. Confocal microscopy images at 7dpi of inoculated *N. benthamiana* leaf cells expressing 1a:RFP and GFP:2a transiently. (A) RFP was fused to C-terminus of 1a. 1a:RFP is visible in intracellular vesicle-like structures along the vacuolar membranes (tonoplasts). (B) GFP was fused to N terminus of 2a. GFP:2a proteins were detected in the cytoplasm and the vesicle-like structures on the vacuolar membranes

B

pCMV-GFP:2a



3. Candidate host factors interacting with CMV viral proteins were found by using Co-IP and LC-MS/MS

To investigate the host proteins that interact with CMV viral protein 2a, Co-immunoprecipitation (Co-IP) and liquid chromatography-tandem mass spectrometry (LC-MS/MS) analysis were performed. pCMV-FLAG:2a, pCMV-R1 and pCMV-R3 constructs were agroinfiltrated into *N. benthamiana* leaves ($OD_{600}=0.7$) together. At 11 dpi, infiltrated leaf tissues were ground in protein extraction buffer followed by centrifugation to remove the cell debris, the supernatant was then incubated with anti-FLAG antibody-coupled magnetic agarose beads. Proteins were eluted from the FLAG beads. Western blot analysis was performed to validate the Co-IP reactions and confirmed that FLAG-2a was successfully pulled down with the FLAG-specific antibodies. SDS-PAGE gel analysis was also performed with co-immunoprecipitated products. (Figure. 4A and 4B). The bands above 130kDa in FLAG:2a lane in western blot were excised from the SDS-PAGE gel for subtractive profiling. It is possibly that FLAG:2a proteins are in the complex with other proteins. We tried to identify novel host proteins which are only found in FLAG:2a complexes by comparing with the same region in CMV lane. In addition, the distinctly separated bands compared to other lanes were also excised from the gel and subjected to LC-MS/MS analysis. The result showed that several host proteins including glyceraldehyde-3-phosphate dehydrogenase-A (GAPDH-A) and eukaryotic translation initiation factor 4A (eIF4A) were identified with high MASCOT scores (Figure. 4C).

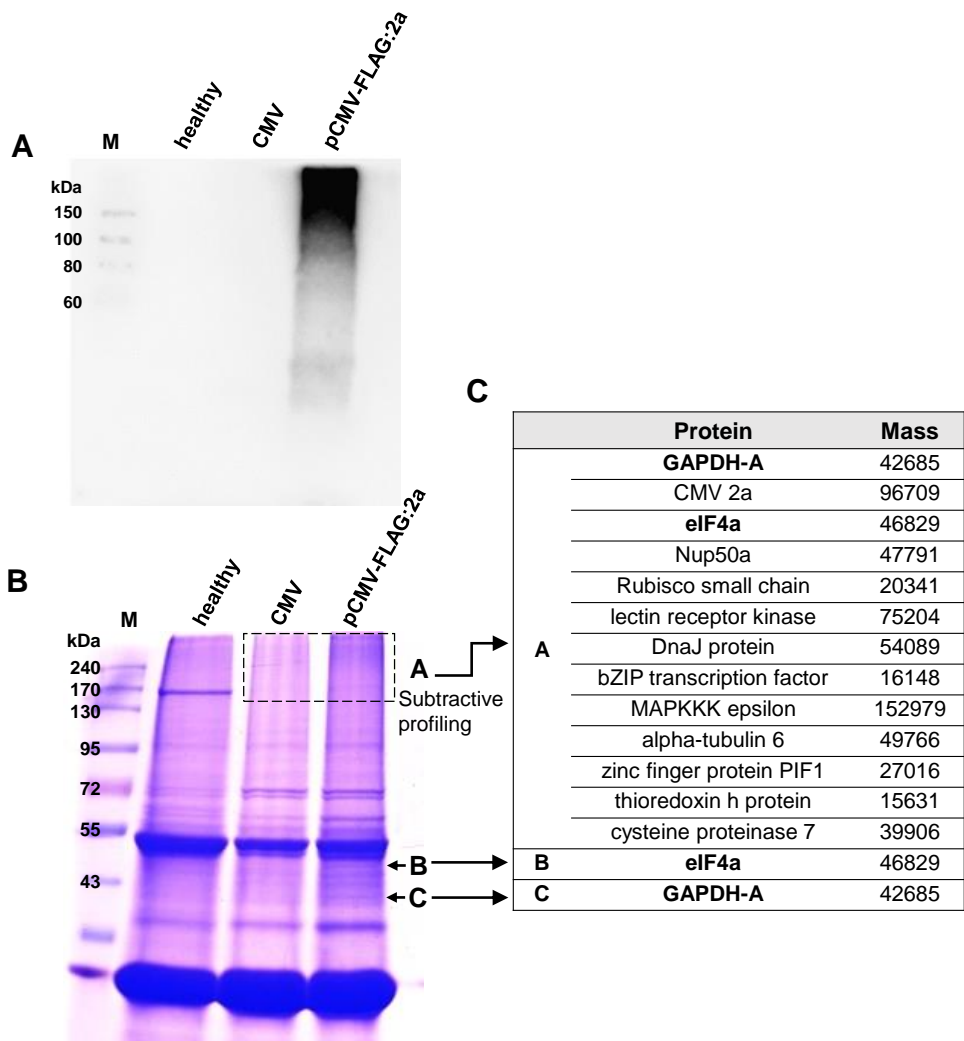


Figure 4. Screening for host factors interacting with CMV 2a protein using Co-IP and LC-MS/MS). CMV (wild type) and CMV (pCMV-FLAG:2a) constructs were agro-infiltrated on the leaves of *N. benthamiana* ($OD_{600} = 0.7$). The upper leaves with symptoms at 11 dpi were extracted and subjected to immunoprecipitation using anti-Flag antibody-conjugated agarose beads. (A) Western blot and (B) SDS-PAGE gel analysis were performed with co-immunoprecipitated products. The bands above 130kDa in FLAG:2a lane detected in western blot were excised for subtractive profiling. The bands at the same region in CMV lane was used as a negative control. In addition, the distinctly separated bands compared to other lanes were also excised from the gel and subjected to LC-MS/MS analysis. (C) List of Candidate Proteins identified by LC-MS/MS

4. Analysis of Differentially expressed genes(DEGs) in response to CMV and/or BBWV2 infection

Interacting between viral components and host factors would cause an alteration in the plant physiology resulting in the development of symptoms (Pallas & Antonio, 2011). Investigating host factors which were highly regulated during CMV infection could help us to understand the molecular mechanisms related to the distinct symptoms induced by CMV. In addition, manipulating important host genes associated CMV infection process will be able to be one of the methods to reduce symptom severity or prevent the CMV infection. In this study, we investigated the infection of pepper ‘Shinhong’ in three different infection condition, CMV, BBWV2 and co-infection, to examine symptom-specific host transcriptome responses. CMV and BBWV2 induce very distinct symptoms in pepper (Figure. 5, Table. 1). Whereas CMV induced stunted growth, leaf size reduction, mosaic and yellowing, BBWV2 infection resulted in veinal chlorosis, leaf malformation, yellowing. In addition, the pepper plants co-infected with CMV and BBWV2 showed severe integrative symptoms compared to each virus infection state (Table. 1).

To identify pepper candidate genes for response to CMV infection, healthy, CMV, BBWV2, and CMV+BBWV2 transcriptome profiles were analyzed. First, the expression level of each gene was normalized as clean reads. Then, the DEGs were determined by comparing gene expressed in CMV-infected plant samples with those from healthy plants with the $p\text{-value} \leq 0.01$ and \log_2 Fold change ≥ 1 or ≤ -1 (Table. 2). We obtained 515 DEGs in response to CMV infection. 315 transcripts were induced, and 200 were repressed by CMV (Figure. 6A). A comparison among DEGs upon CMV, BBWV2 and CMV+BBWV2 infection identified only 31 genes induced and 9 genes repressed specifically in CMV infection (Figure. 6C). The analysis also revealed that the number of induced transcripts was greater than repressed transcripts in all infection situations (Figure. 6B).

To observe the gene expression patterns in each sample, the magnitude distribution of the DEGs was illustrated by MA plot analysis (Figure. 6C). The MA plots showed that pepper gene expression pattern was affected a lot by co-infection of two viruses enhanced changes in the gene expression pattern (Figure. 6C). In addition, a hierarchical clustering of the total DEGs identified six groups according to the expression patterns in each infection condition (Figure. 6D). These results indicated that the majority of genes in response to CMV were unique and CMV symptom in pepper might be due to the different expression levels of these DEGs.



Figure 5. Comparison of Symptoms of CMV, BBWV2 and CMV+BBWV2. Symptoms induced by CMV, BBWV2, CMV+BBWV2 at 20 days post-inoculation (dpi) by sap infection. BBWV2 and CMV induced distinct symptoms (Table 2.) on *Nicotiana benthamiana*. cv. Shinhong plants.

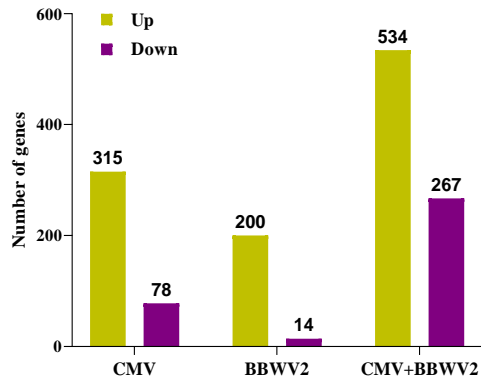
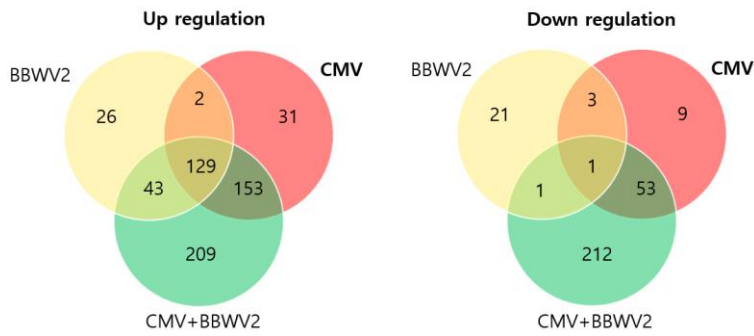
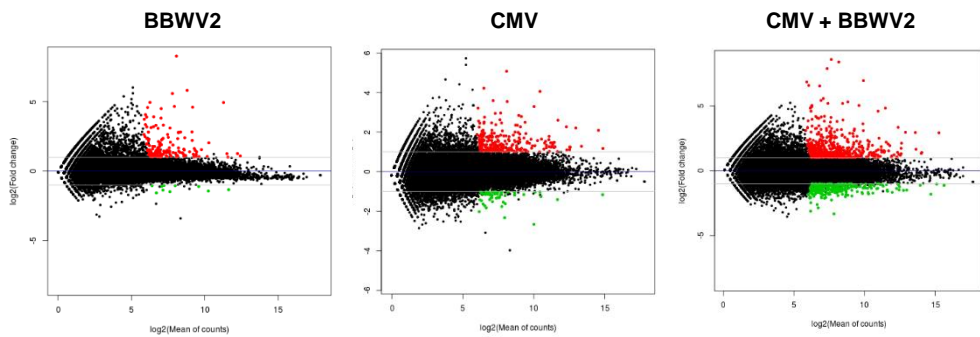
Table 1. Symptoms induced by CMV, BBWV2 and CMV+BBWV2 in pepper cv. ‘Shinhong’

| Virus | Broad bean wilt virus 2 (BBWV2) | Cucumber Mosaic Virus (CMV) | Co-infection (CMV and BBWV2) |
|-----------------|--|------------------------------------|-------------------------------------|
| | Veinal chlorosis | Stunting | Severe stunting |
| Symptoms | Leaf malformation | Leaf size reduction | Severe leaf size reduction |
| | Yellowing | Mosaic | |

Table 2. Read statistics for RNA Sequencing of pepper plants in response to infection with CMV, BBWV2 and CMV+BBWV2

| Index | Healthy | CMV | BBWV2 | CMV+BBWV2 |
|------------------------------|----------------|---------------|---------------|------------------|
| No. of trimmed reads(%) | 80,988,234 | 89,158,100 | 85,958,586 | 90,338,300 |
| | 90.73% | 91.55% | 91.83% | 92.79% |
| No. of mapped reads(%) | 75,175,224 | 82,327,921 | 71,890,360 | 63,793,145 |
| | 92.82% | 92.34% | 83.63% | 70.62% |
| No. of mapped nucleotides(%) | 6,848,712,056 | 7,526,945,055 | 6,592,273,522 | 5,926,536,579 |
| | 92.81% | 92.55% | 83.62% | 70.62% |
| Average coverage | 175.00 | 192.33 | 168.45 | 151.44 |

Figure 6. Comparison of differentially expressed genes (DEGs) in response to infection with CMV or/and BBWV2. (A) The number of up- or down-regulated DEGs upon each virus infection. The DEGs were identified by comparing the virus infected samples to the healthy sample using a twofold change in expression with a false discovery rate (FDR) ≤ 0.01 and mean of read count ≥ 1000 as cutoffs. Green and purple bars indicate the numbers of up- and down-regulated DEGs, respectively. (B) Venn diagrams display the number of up- or down-regulated DEGs in CMV and/or BBWV2 infection conditions. (C) The MA-plots of DEGs. Each dots represents a gene. The x axis indicates the normalized mean of read counts and the y axis indicates the log₂ fold change of normalized counts. The red and green dots represent up- and down-regulated DEGs, respectively, obtained in this study. (D) Hierarchical clustering of DEGs obtained from CMV and/or BBWV2 infection conditions. Red and green colors indicate the numbers of up- and down-regulation, respectively. The linear graphs show the expression patterns of each cluster.

A**B****C**

D

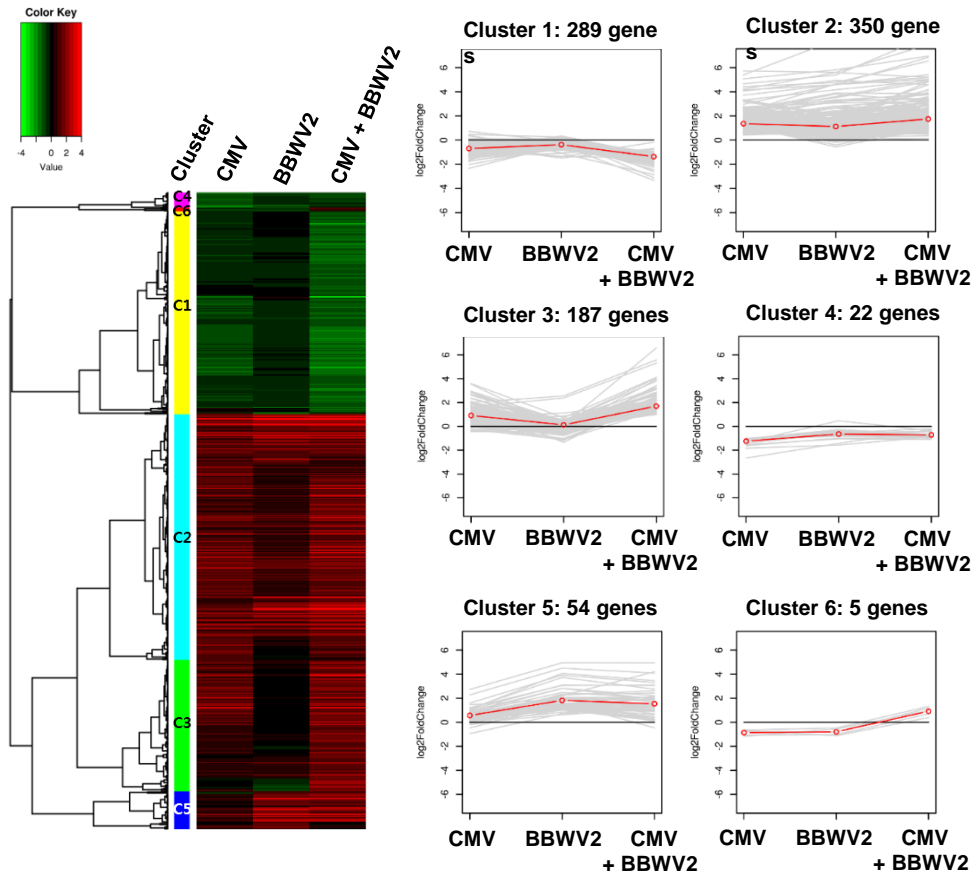


Table 3. Top 20 up and down DEGs in response to infection with CMV

| Gene | Seq. Description | log2 fold change | | |
|-----------------------------|---|------------------|-------|---------------|
| | | CMV | BBWV2 | CMV+ BBWV2 |
| Up regulation | | | | |
| CA.PGAv.1.6.scaffold631.48 | Ripening-related protein grip22 | 5.08 | 5.82 | 6.95 |
| CA.PGAv.1.6.scaffold674.24 | ATP binding protein, putative | 4.22 | 5.59 | 5.20 |
| CA.PGAv.1.6.scaffold1405.6 | Glycine-rich protein | 4.06 | 4.94 | 4.59 |
| CA.PGAv.1.6.scaffold291.8 | AP2/ERF domain-containing transcription factor | 3.59 | 0.73 | 4.11 |
| CA.PGAv.1.6.scaffold889.4 | NEP-TC | 3.55 | -0.21 | 3.92 |
| CA.PGAv.1.6.scaffold939.24 | Antimicrobial peptide 1 | 3.29 | 1.57 | 4.83 |
| CA.PGAv.1.6.scaffold575.23 | protein ECERIFERUM 1 | 3.21 | 2.17 | 4.15 |
| CA.PGAv.1.6.scaffold890.65 | acidic endochitinase pcht28-like | 2.97 | 4.60 | 5.04 |
| CA.PGAv.1.6.scaffold21.10 | Alkaline alpha-galactosidase seed imbibition protein | 2.95 | 0.45 | 3.80 |
| CA.PGAv.1.6.scaffold588.80 | DNA binding protein, putative | 2.85 | -0.16 | 3.22 |
| CA.PGAv.1.6.scaffold1306.1 | Pro-hevin | 2.79 | 1.67 | 3.62 |
| CA.PGAv.1.6.scaffold1110.29 | Serine/threonine-protein kinase | 2.75 | 3.08 | 3.19 |
| CA.PGAv.1.6.scaffold1134.16 | hypothetical protein T459_22339 | 2.62 | 0.24 | 2.71 |
| CA.PGAv.1.6.scaffold13678.1 | antifungal protein | 2.60 | 1.22 | 3.35 |
| CA.PGAv.1.6.scaffold889.10 | Pyruvate orthophosphate dikinase | 2.56 | 0.67 | 2.34 |
| CA.PGAv.1.6.scaffold370.26 | PREDICTED: cysteine proteinase RD21a-like | 2.51 | 1.99 | 2.34 |
| CA.PGAv.1.6.scaffold423.30 | Phosphoethanolamine n-methyltransferase, putative | 2.50 | 2.21 | 3.10 |
| CA.PGAv.1.6.scaffold254.2 | PREDICTED: bidirectional sugar transporter SWEET15-like | 2.47 | 0.93 | 1.27 |
| CA.PGAv.1.6.scaffold1611.1 | PREDICTED: endochitinase-like | 2.46 | 1.55 | 3.17 |
| CA.PGAv.1.6.scaffold241.41 | R2r3-myb transcription factor, putative | 2.45 | 1.33 | 1.46 |
| Down regulation | | | | |
| CA.PGAv.1.6.scaffold484.97 | Soluble diacylglycerol acyltransferase | -2.66 | -1.43 | -0.28 |
| CA.PGAv.1.6.scaffold5.23 | PREDICTED: acanthoscurrin-1-like isoform X1 | -2.33 | -0.43 | -3.32 |
| CA.PGAv.1.6.scaffold303.33 | Caffeic acid 3-O-methyltransferase | -2.02 | -0.62 | -2.03 |
| CA.PGAv.1.6.scaffold702.9 | Phospholipase A1-Ilgamma-like | -1.83 | -1.57 | -0.88 |
| CA.PGAv.1.6.scaffold688.1 | PREDICTED: acanthoscurrin-1-like isoform X1 | -1.76 | -0.39 | -2.25 |
| CA.PGAv.1.6.scaffold1217.13 | hypothetical protein T459_00549 | -1.72 | -0.74 | -1.78 |
| CA.PGAv.1.6.scaffold410.33 | germin-like protein subfamily 1 member 11 | -1.64 | 0.18 | -3.11 |
| CA.PGAv.1.6.scaffold132.22 | Linalool/nerolidol synthase | -1.62 | -0.98 | -0.95 |
| CA.PGAv.1.6.scaffold1174.1 | Terpene synthase | -1.54 | -1.05 | -1.09 |
| CA.PGAv.1.6.scaffold1559.2 | Omega-3 fatty acid desaturase | -1.51 | -0.66 | -1.81 |
| CA.PGAv.1.6.scaffold1030.35 | ATP binding protein, putative | -1.47 | -0.52 | -2.07 |
| CA.PGAv.1.6.scaffold1129.9 | Kinesin-like protein NACK1 | -1.42 | -0.58 | -1.01 |
| CA.PGAv.1.6.scaffold589.2 | Elongation factor 1-alpha | -1.41 | -0.17 | -1.59 |
| CA.PGAv.1.6.scaffold861.41 | Proteinase inhibitor type-2 CEV157 | -1.41 | 0.33 | -2.61 |
| CA.PGAv.1.6.scaffold569.23 | Cytochrome P450 | -1.34 | -0.40 | -2.11 |
| CA.PGAv.1.6.scaffold771.42 | Cucumisun, putative | -1.33 | -0.61 | -2.06 |
| CA.PGAv.1.6.scaffold322.14 | PREDICTED: serine carboxypeptidase II-3-like | -1.32 | -1.09 | -2.86 |
| CA.PGAv.1.6.scaffold572.61 | PRP1 | -1.32 | 0.47 | -0.38 |
| CA.PGAv.1.6.scaffold916.12 | Leucine-rich repeat protein kinase | -1.32 | -0.44 | -1.50 |
| CA.PGAv.1.6.scaffold198.27 | glycine-rich cell wall structural protein 1-like | -1.27 | -0.82 | -1.74 |

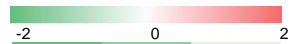


Table 4. Top 20 up and down DEGs in response to infection with BBWV2

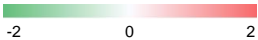
| Gene | Seq. Description | log2 fold change | | |
|--|--|------------------|-------|---------------|
| | | CMV | BBWV2 | CMV+ BBWV2 |
| Up regulation | | | | |
| CA.PGAv.1.6.scaffold608.26 | PREDICTED: pathogenesis-related leaf protein 4-like | 5.40 | 8.29 | 8.38 |
| CA.PGAv.1.6.scaffold631.48 | Ripening-related protein grip22 | 5.08 | 5.82 | 6.95 |
| CA.PGAv.1.6.scaffold674.24 | ATP binding protein, putative | 4.22 | 5.59 | 5.20 |
| CA.PGAv.1.6.scaffold58.30 | PREDICTED: probable mitochondrial chaperone BCS1-A-like | 2.73 | 4.95 | 4.94 |
| CA.PGAv.1.6.scaffold1405.6 | Glycine-rich protein | 4.06 | 4.94 | 4.59 |
| CA.PGAv.1.6.scaffold890.64 | basic chitinase | 2.30 | 4.66 | 5.19 |
| CA.PGAv.1.6.scaffold890.65 | basic chitinase | 2.97 | 4.60 | 5.04 |
| CA.PGAv.1.6.scaffold575.21 | PREDICTED: protein ECERIFERUM 1-like | 4.14 | 4.59 | 5.42 |
| CA.PGAv.1.6.scaffold79.50 | Tau class glutathione transferase GSTU15 | 2.28 | 4.50 | 4.09 |
| CA.PGAv.1.6.scaffold793.11 | E8 protein homolog | 1.07 | 4.07 | 3.46 |
| CA.PGAv.1.6.scaffold753.4 | PREDICTED: probable mitochondrial chaperone BCS1-B-like | 1.60 | 3.92 | 3.31 |
| CA.PGAv.1.6.scaffold628.31 | Abc transporter, putative | 2.50 | 3.90 | 3.85 |
| CA.PGAv.1.6.scaffold1537.4 | probable LRR receptor-like serine/threonine-protein kinase | 2.35 | 3.82 | 3.26 |
| CA.PGAv.1.6.scaffold823.8 | Ammonium transporter | 1.15 | 3.73 | 2.75 |
| CA.PGAv.1.6.scaffold242.12 | Phenazine biosynthesis PhzC/PhzF protein | 2.46 | 3.35 | 3.35 |
| CA.PGAv.1.6.scaffold1134.9 | PREDICTED: broad-range acid phosphatase DET1-like | 1.81 | 3.32 | 3.75 |
| CA.PGAv.1.6.scaffold1134.7 | PREDICTED: broad-range acid phosphatase DET1-like | 1.78 | 3.30 | 3.82 |
| CA.PGAv.1.6.scaffold577.9 | CYP72A53v2 | 2.22 | 3.20 | 3.47 |
| CA.PGAv.1.6.scaffold628.32 | PREDICTED: ABC transporter A family member 2-like | 2.22 | 3.19 | 3.45 |
| CA.PGAv.1.6.scaffold608.6 | Hcr9-Avr4-par1 | 2.28 | 3.13 | 2.98 |
|  | | | | |
| Down regulation | | | | |
| CA.PGAv.1.6.scaffold702.9 | alpha/beta-Hydrolases superfamily protein | -1.83 | -1.57 | -0.88 |
| CA.PGAv.1.6.scaffold837.4 | 42kDa chitin-binding protein | -0.47 | -1.48 | -0.69 |
| CA.PGAv.1.6.scaffold484.97 | Soluble diacylglycerol acyltransferase | -2.66 | -1.43 | -0.28 |
| CA.PGAv.1.6.scaffold1410.1 | Xenotropic and polytropic murine leukemia virus receptor ids-4, putative | -0.40 | -1.37 | -0.17 |
| CA.PGAv.1.6.scaffold1397.2 | Heat shock protein, putative | -0.86 | -1.34 | -1.48 |
| CA.PGAv.1.6.scaffold361.18 | PREDICTED: uncharacterized protein LOC107845694 | -0.66 | -1.11 | 0.39 |
| CA.PGAv.1.6.scaffold322.14 | PREDICTED: serine carboxypeptidase II-3-like | -1.32 | -1.09 | -2.86 |
| CA.PGAv.1.6.scaffold1130.2 | PREDICTED: UPF0301 protein Cpha266_0885-like isoform 1 | 0.42 | -1.05 | -0.78 |
| CA.PGAv.1.6.scaffold1174.1 | Terpene synthase | -1.54 | -1.05 | -1.09 |
| CA.PGAv.1.6.scaffold293.20 | hypothetical protein T459_02727 | -1.06 | -1.03 | 0.70 |

Table 5. Top 20 up and down DEGs in response to infection with CMV+BBWV2

| Gene | Seq. Description | log2 fold change | | |
|--|--|------------------|-------|-----------|
| | | CMV | BBWV2 | CMV+BBWV2 |
| Up regulation | | | | |
| CA.PGAv.1.6.scaffold557.2 | Endochitinase | 4.66 | 5.39 | 8.58 |
| CA.PGAv.1.6.scaffold608.26 | PREDICTED: pathogenesis-related leaf protein 4-like | 5.40 | 8.29 | 8.38 |
| CA.PGAv.1.6.scaffold890.60 | Detected protein of confused Function | 5.73 | 5.61 | 7.89 |
| CA.PGAv.1.6.scaffold631.48 | Ripening-related protein grip22 | 5.08 | 5.82 | 6.95 |
| CA.PGAv.1.6.scaffold981.1 | Pathogenesis related protein-5 | 3.72 | 4.60 | 6.85 |
| CA.PGAv.1.6.scaffold379.2 | PREDICTED: protein kinase 2B, chloroplastic-like | 2.87 | 0.16 | 6.58 |
| CA.PGAv.1.6.scaffold6.29 | PREDICTED: probable WRKY transcription factor 51-like | 4.42 | 4.77 | 6.54 |
| CA.PGAv.1.6.scaffold164.15 | Mitochondrial small heat shock protein | 2.00 | 2.55 | 5.57 |
| CA.PGAv.1.6.scaffold575.21 | PREDICTED: protein ECERIFERUM 1-like | 4.14 | 4.59 | 5.42 |
| CA.PGAv.1.6.scaffold1367.3 | Mitochondrial small heat shock protein | 1.64 | 2.38 | 5.31 |
| CA.PGAv.1.6.scaffold674.24 | ATP binding protein, putative | 4.22 | 5.59 | 5.20 |
| CA.PGAv.1.6.scaffold890.64 | basic chitinase | 2.30 | 4.66 | 5.19 |
| CA.PGAv.1.6.scaffold624.33 | PREDICTED: multiprotein-bridging factor 1c-like | 2.26 | 3.61 | 5.04 |
| CA.PGAv.1.6.scaffold890.65 | basic chitinase | 2.97 | 4.60 | 5.04 |
| CA.PGAv.1.6.scaffold58.30 | PREDICTED: probable mitochondrial chaperone BCS1-A-like | 2.73 | 4.95 | 4.94 |
| CA.PGAv.1.6.scaffold206.16 | Beta-1,3-glucanase 28 (Precursor) | 3.31 | 4.17 | 4.93 |
| CA.PGAv.1.6.scaffold845.22 | hypothetical protein T459_04045 | 2.62 | 3.52 | 4.84 |
| CA.PGAv.1.6.scaffold939.24 | Antimicrobial peptide 1 | 3.29 | 1.57 | 4.83 |
| CA.PGAv.1.6.scaffold345.2 | PREDICTED: non-specific lipid-transfer protein 2-like | 3.19 | 1.97 | 4.59 |
| CA.PGAv.1.6.scaffold1405.6 | Glycine-rich protein | 4.06 | 4.94 | 4.59 |
|  | | | | |
| Down regulation | | | | |
| CA.PGAv.1.6.scaffold5.23 | PREDICTED: acanthoscurrin-1-like isoform X1 | -2.33 | -0.43 | -3.32 |
| CA.PGAv.1.6.scaffold410.33 | RmlC-like cupins superfamily protein | -1.64 | 0.18 | -3.11 |
| CA.PGAv.1.6.scaffold322.14 | PREDICTED: serine carboxypeptidase II-3-like | -1.32 | -1.09 | -2.86 |
| CA.PGAv.1.6.scaffold861.41 | Proteinase inhibitor type-2 CEV157 | -1.41 | 0.33 | -2.61 |
| CA.PGAv.1.6.scaffold585.34 | ER glycerol-phosphate acyltransferase | -0.90 | -0.23 | -2.46 |
| CA.PGAv.1.6.scaffold688.1 | PREDICTED: acanthoscurrin-1-like isoform X1 | -1.76 | -0.39 | -2.25 |
| CA.PGAv.1.6.scaffold569.23 | Cytochrome P450 | -1.34 | -0.40 | -2.11 |
| CA.PGAv.1.6.scaffold579.7 | ATP synthase CF1 epsilon subunit | -1.15 | -0.43 | -2.10 |
| CA.PGAv.1.6.scaffold585.54 | PREDICTED: protodermal factor 1-like | -0.96 | -0.38 | -2.08 |
| CA.PGAv.1.6.scaffold1030.35 | ATP binding protein, putative | -1.47 | -0.52 | -2.07 |
| CA.PGAv.1.6.scaffold771.42 | Cucumisins, putative | -1.33 | -0.61 | -2.06 |
| CA.PGAv.1.6.scaffold303.33 | Caffeic acid 3-O-methyltransferase | -2.02 | -0.62 | -2.03 |
| CA.PGAv.1.6.scaffold349.9 | Lanceolate | -0.98 | -0.58 | -2.02 |
| CA.PGAv.1.6.scaffold1392.3 | Dihydroliipoamide dehydrogenase, putative | -0.96 | -0.77 | -2.00 |
| CA.PGAv.1.6.scaffold778.2 | Tuber-specific and sucrose-responsive element binding factor | -1.07 | -0.58 | -1.98 |
| CA.PGAv.1.6.scaffold919.19 | Gland-specific fatty acyl-CoA reductase 1 | -1.16 | -0.53 | -1.94 |
| CA.PGAv.1.6.scaffold3.26 | Ribulose bisphosphate carboxylase large chain | -1.12 | -0.35 | -1.91 |
| CA.PGAv.1.6.scaffold1389.21 | Detected protein of unknown function | -0.68 | -0.22 | -1.87 |
| CA.PGAv.1.6.scaffold1078.7 | GMC-type oxidoreductase, putative | -1.13 | -0.79 | -1.87 |
| CA.PGAv.1.6.scaffold100.35 | hypothetical protein T459_02427 | -0.83 | -0.38 | -1.86 |

5. Gene ontology (GO) terms and enrichment analysis of identified DEGs upon CMV infection

For a better understanding of the DEGs involved in response to infection with CMV, the functional classes of DEGs were subjected to gene ontology (GO) analysis. A total of 98, 197, and 230 GO terms were significantly enriched by infection with CMV, BBWV2, and CMV+BBWV2, respectively (Fig. 7A). Among three infection conditions, 31 and 0 GO terms were commonly identified for up- and down-regulated DEGs (Figure. 7B). To focus on the CMV infection environment, we performed GO enrichment analysis in biological process category using REVIGO and agriGO. Gene ontology scatterplot was constructed with REVIGO in R (Figure. 8A). The enriched GO terms for up-regulated DEGs included response to stimulus (GO:0050896), response to stress (GO:0006950), response to chemical (GO:0050896), response to external stimulus (GO:0009605) (Figure. 8A and 8B). Many of the DEGs related to stress response were particularly significance in the REVIGO and agriGO singular enrichment analysis (Figure. 8B). The GO terms enriched for the down-regulated DEGs contained cell cycle (GO:0015979), DNA replication (GO:0006260), cell division (GO:0051301), DNA conformation change (GO:0071103) (Figure. 9A and 9B). As listed in Figure 9B, most of the cell cycle related genes were particularly significance in CMV infection. These data suggest that during symptom development, pepper plants respond to CMV infection by expressing stress response related genes and by suppressing cell cycle related genes. DEGs involved in cell cycle such as inactive receptor kinase (PUTATIVE KINASE), cyclin-D3 (CYCD3), cyclin-A1 (CYCA1), cyclin-A2 (CYCA2), condensin complex subunit 1 (CAP-D2), fatty acyl-coA reductase 3-like isoform X1 (CER4) were repressed during CMV infection (Figure. 10). The down-regulation of the genes related to the cell cycle is likely to be related to stunting and leaf size reduction induced by CMV.

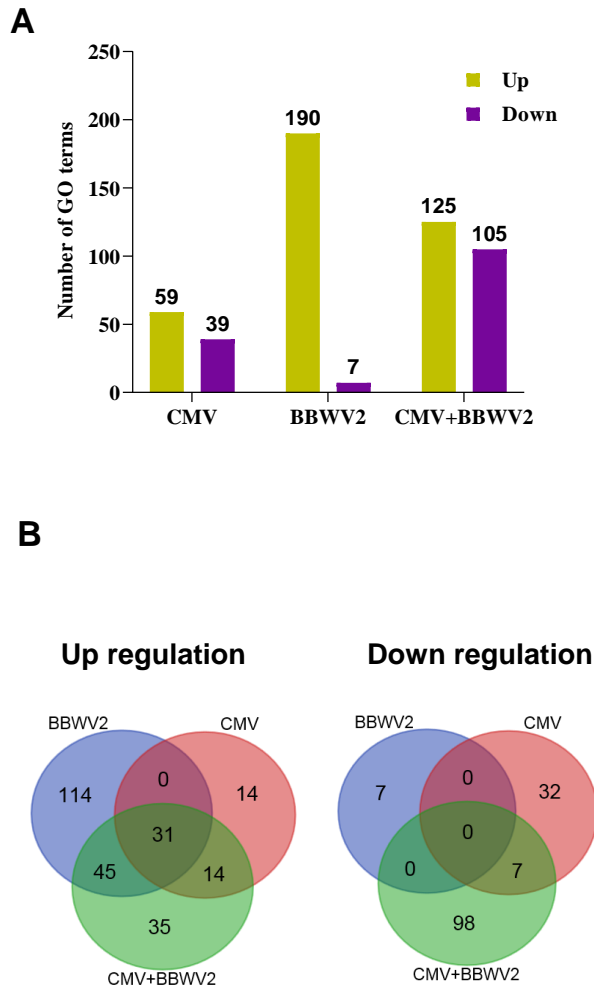
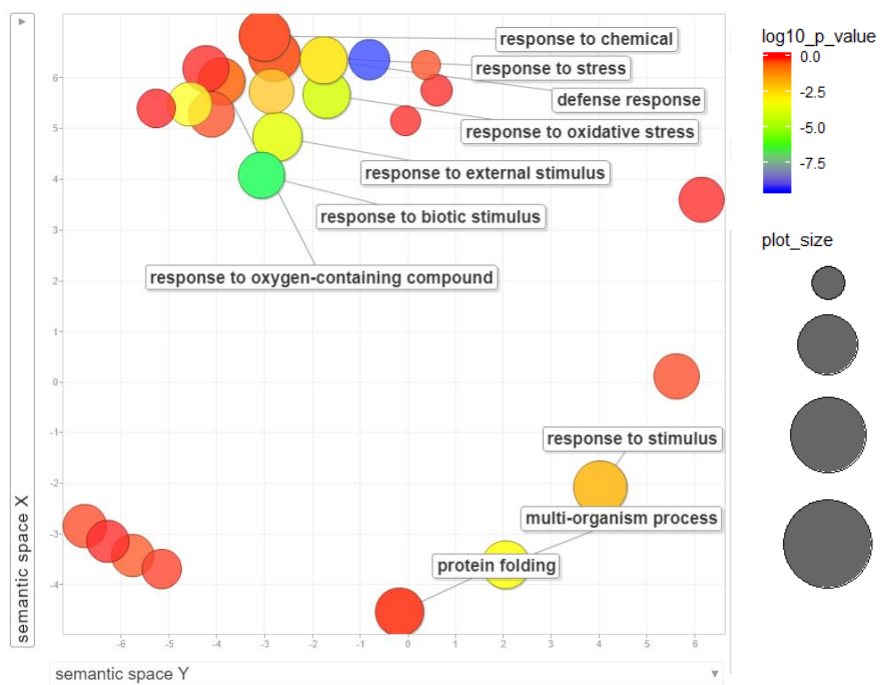


Figure 7. Gene Ontology (GO) terms analysis in CMV infection (A) The number of up- or down-regulated GO terms in response to infection with CMV or/and BBWV2. Green and purple bars indicate the numbers of up- and down-regulated DEGs, respectively. (B) Venn diagrams display the number of up- or down-regulated GO terms in CMV and/or BBWV2 infection conditions.

Figure 8. GO enrichment analysis of up-regulated DEG (A) GO enrichment analysis in biological process category using REVIGO. The scatter plot showing the significance of the GO terms for DEGs in a two-dimensional space derived by applying multi-dimensional scaling to a matrix of GO term semantic similarities. Bubble color indicates the p-value for the false discovery rates (FDR). The circle size represents the frequency of the GO term. (B) Top 10 GO terms enriched with up-regulated DEGs after CMV infection. (C) Hierarchical tree graph of overrepresented GO terms using up-regulated DEGs in biological process category upon CMV infection using agriGO. Significant terms (FDR < 0.05) are colored. The degree of color saturation of a box is positively correlated to the enrichment level of the term.

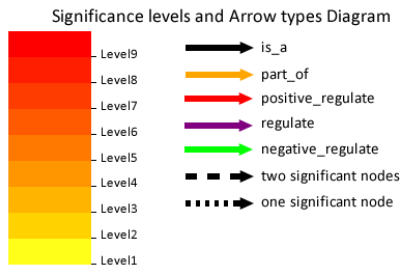
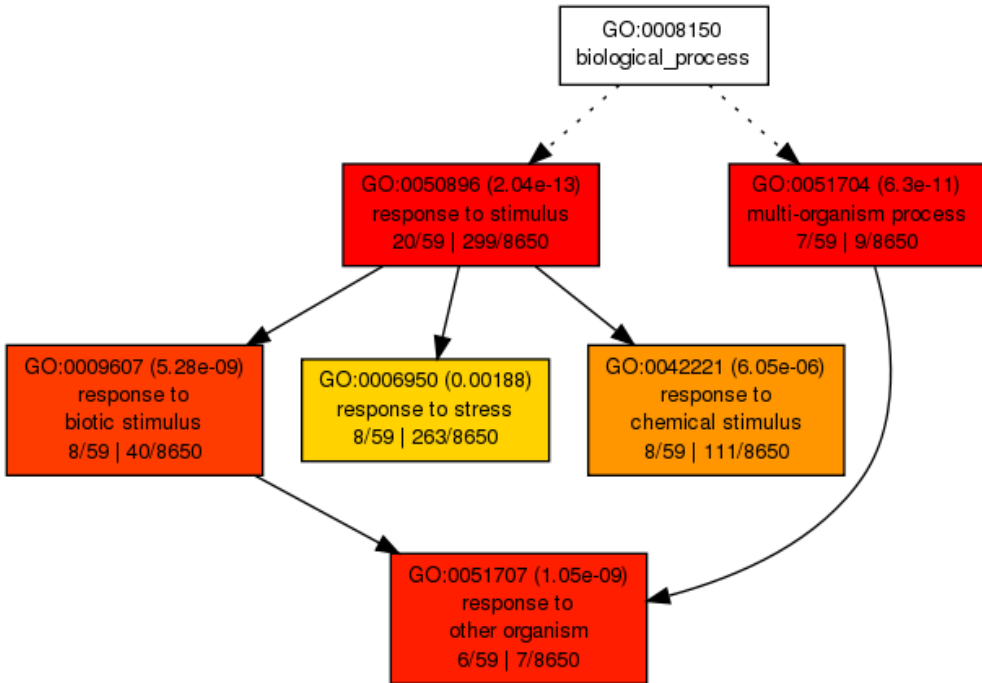
A



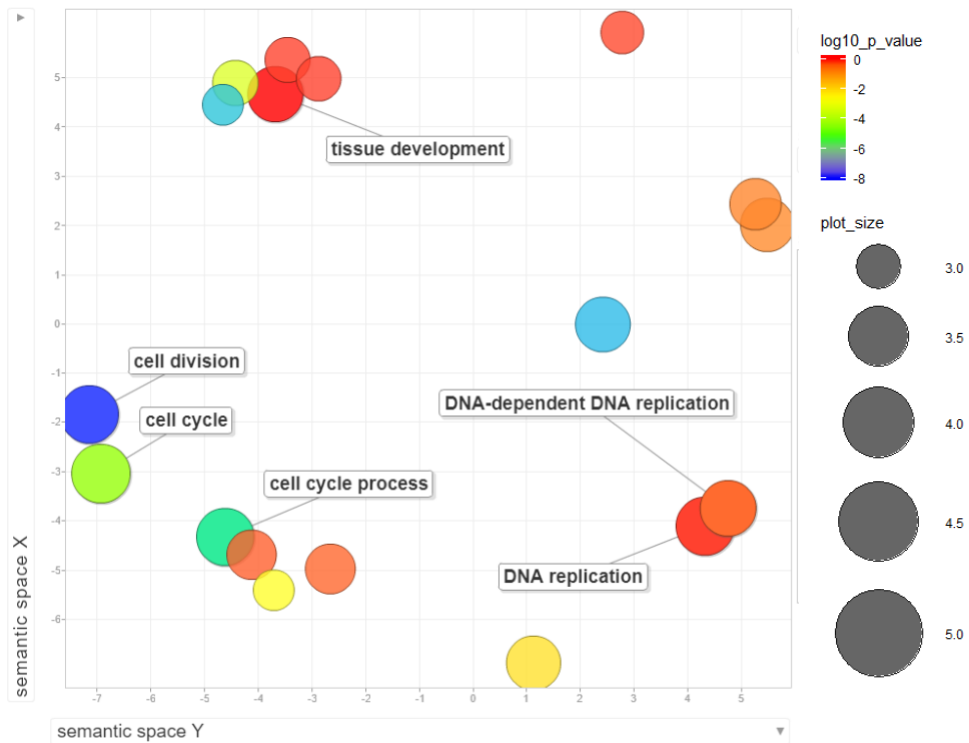
B

| term_ID | description | frequency_% |
|------------|--|-------------|
| GO:0050896 | response to stimulus | 12.21% |
| GO:0006950 | response to stress | 4.58% |
| GO:0042221 | response to chemical | 3.07% |
| GO:0009605 | response to external stimulus | 1.37% |
| GO:0006457 | protein folding | 0.90% |
| GO:0051704 | multi-organism process | 0.75% |
| GO:0006979 | response to oxidative stress | 0.58% |
| GO:0006952 | defense response | 0.57% |
| GO:1901700 | response to oxygen-containing compound | 0.50% |
| GO:0009607 | response to biotic stimulus | 0.34% |

C



A



B

| term_ID | description | frequency-% |
|------------|-------------------------------|-------------|
| GO:0007049 | cell cycle | 1.89% |
| GO:0006260 | DNA replication | 1.58% |
| GO:0051301 | cell division | 1.23% |
| GO:0071103 | DNA conformation change | 1.08% |
| GO:0022402 | cell cycle process | 1.05% |
| GO:0006261 | DNA-dependent DNA replication | 0.58% |
| GO:0000278 | mitotic cell cycle | 0.56% |
| GO:0051726 | regulation of cell cycle | 0.55% |
| GO:1903047 | mitotic cell cycle process | 0.51% |
| GO:0009888 | tissue development | 0.49% |

C

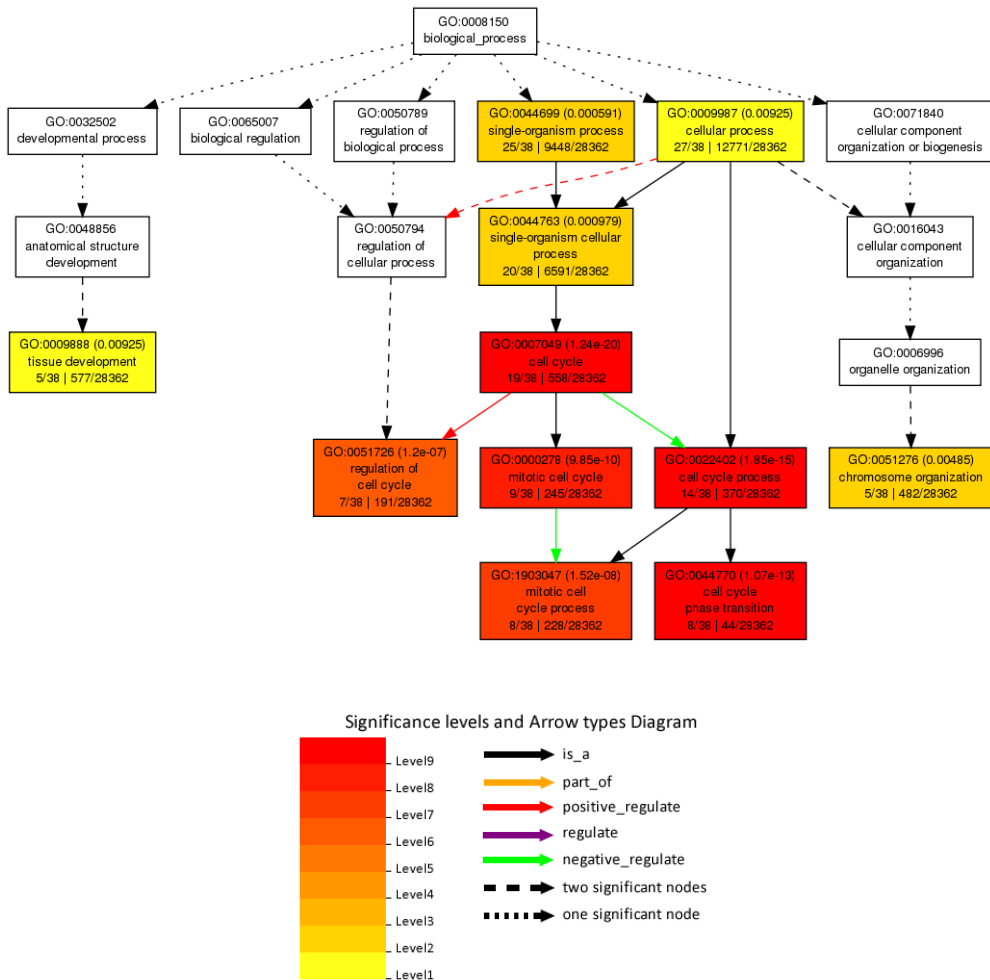


Figure 9. GO enrichment analysis of down-regulated DEGs. (A) GO enrichment analysis of down-regulated DEGs in biological process category using REVIGO. Bubble color indicates the p-value for the false discovery rates (FDR). The circle size represents the frequency of the GO term. (B) Top 10 GO terms enriched with down-regulated DEGs after CMV infection. (C) Hierarchical tree graph of overrepresented GO terms using down-regulated DEGs in biological process category upon CMV infection using agriGO. Significant terms (FDR < 0.05) are colored. The degree of color saturation of a box is positively correlated to the enrichment level of the term.

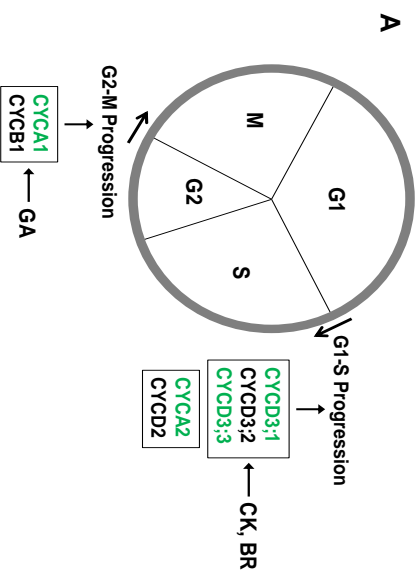


Figure. 10. Regulation of the genes associated with Cell cycle regulation upon CMV infection in pepper (A) Cell division cycle and key enzymes and hormones relate to cell cycle checkpoint (B) The DEGs associated with cell cycle regulation. Red and Green indicate up- and down-regulation, respectively.

| Gene | Seq. Description | log2 fold change | | | Arabidopsis homolog | TAIR symbol |
|-----------------------------|--|------------------|-------|------------|---------------------|-----------------|
| | | CMV | BBWV2 | CMV+ BBWV2 | | |
| CA.PGAy.1.6.scaffold1030.35 | probable inactive receptor kinase At5g67200 | -1.47 | -0.52 | -2.07 | AT3G50230 | PUTATIVE KINASE |
| CA.PGAy.1.6.scaffold1129.9 | kinesin-like protein NACK1 | -1.42 | -0.58 | -1.01 | AT1G18370 | HINKEL |
| CA.PGAy.1.6.scaffold191.19 | fatty acyl-CoA reductase 3-like isoform X1 | -1.16 | -0.53 | -1.94 | AT4G33790 | CER4 |
| CA.PGAy.1.6.scaffold174.174 | condensin complex subunit 1 | -1.13 | -0.79 | -1.87 | AT3G57060 | CAP-D2 |
| CA.PGAy.1.6.scaffold322.42 | phragmoplast orienting kinesin 2 | -1.12 | -0.33 | -0.84 | AT3G19050 | POK2 |
| CA.PGAy.1.6.scaffold424.35 | putative cyclin-D6-1 | -1.11 | -0.82 | -0.85 | AT4G03270 | CYCD6:1 |
| CA.PGAy.1.6.scaffold1812.1 | cyclin-D3-3-like | -1.08 | -0.70 | -0.70 | AT3G50070 | CYCD3:3 |
| CA.PGAy.1.6.scaffold1231.17 | cyclin-D3-1 | -1.06 | -0.37 | -0.70 | AT4G34160 | CYCD3:1 |
| CA.PGAy.1.6.scaffold668.33 | cellulose synthase-like protein D5 | -1.05 | -0.54 | -0.83 | AT1G02730 | CSLD5 |
| CA.PGAy.1.6.scaffold206.153 | LRR receptor-like serine/threonine-protein kinase ERECTA | -1.02 | -0.41 | -0.68 | AT2G26330 | ER |
| CA.PGAy.1.6.scaffold6.33 | structural maintenance of chromosomes protein 4 | -1.02 | -0.36 | -1.68 | AT5G44700 | GSD2 |
| CA.PGAy.1.6.scaffold48.1 | cyclin-A1-4 isoform X1 | -1.00 | -0.46 | -0.80 | AT1G44110 | CYCA1:1 |
| CA.PGAy.1.6.scaffold199.59 | cyclin-A2-2 | -1.00 | -0.54 | -0.91 | AT5G11300 | CYCA2:2 |



6. Important KEGG pathways influenced by CMV infection

We performed a pathway analysis using KEGG (Kyoto Encyclopedia of Genes and Genomes) to understand the relationship between DEGs and the associated pathways. KEGG pathway enrichment analysis upon CMV infection was performed using orthologs in Arabidopsis genes (TAIR) by DAVID 6.8 (Huang da et al., 2009). Analysis of DEGs by DAVID also revealed that Plant hormone signal transduction, Cysteine and methionine metabolism and Biosynthesis of secondary metabolites were significantly enriched functions (Table 6 and 7).

Cysteine and methionine metabolism and Plant hormone signal transductions were highly related to Ethylene synthesis and signaling pathway. Ethylene is one of the most important hormones in the leaf senescence regulation (Wang et al., 2002). Activation of these pathways seems to be related to accumulation of Ethylene in leaves infected with CMV. DEGs related to Ethylene synthesis and signaling were up-regulated such as SAM synthetase (SAM1), ACC synthetase (ACS) and ACC oxidase (ACO) and negative regulators of Ethylene pathways such as CONSTITUTIVE TRIPLE RESPONSE1 (CTR1) were down-regulated (Figure. 11).

Moreover, some DEGs regulated by CMV were also involved in the Auxin synthesis and signaling pathway (e.g., ALDH4; Aldehyde dehydrogenase), cytokinin synthesis and signaling pathway (e.g., LOG4; LONELY GUY 4), jasmonic acid synthesis and signaling pathway (e.g., RGL2; RGA-like 2) and brassinosteroid (BR) synthesis and signaling pathway (e.g., CAS1; CYCLOARTENOL SYNTHASE 1) (Table. 7). These data indicated that symptom development by CMV infection engages in cross-talk with other plant hormone molecules.

Table 6. KEGG pathway enrichment analysis upon CMV infection by DAVID 6.8

| KEGG Pathway | Count | % | P-Value | FDR |
|---------------------------------------|--------------|----------|----------------|------------|
| Plant hormone signal transduction | 18 | 6.8 | 9.10E-07 | 9.10E-04 |
| Cysteine and methionine metabolism | 11 | 4.1 | 4.00E-06 | 4.00E-03 |
| Biosynthesis of secondary metabolites | 33 | 12.4 | 7.20E-05 | 7.20E-02 |
| ABC transporters | 4 | 1.5 | 6.80E-03 | 6.60E+00 |
| Diterpenoid biosynthesis | 3 | 1.1 | 5.00E-02 | 4.00E+01 |
| Cutin, suberine and wax biosynthesis | 3 | 1.1 | 7.20E-02 | 5.30E+01 |

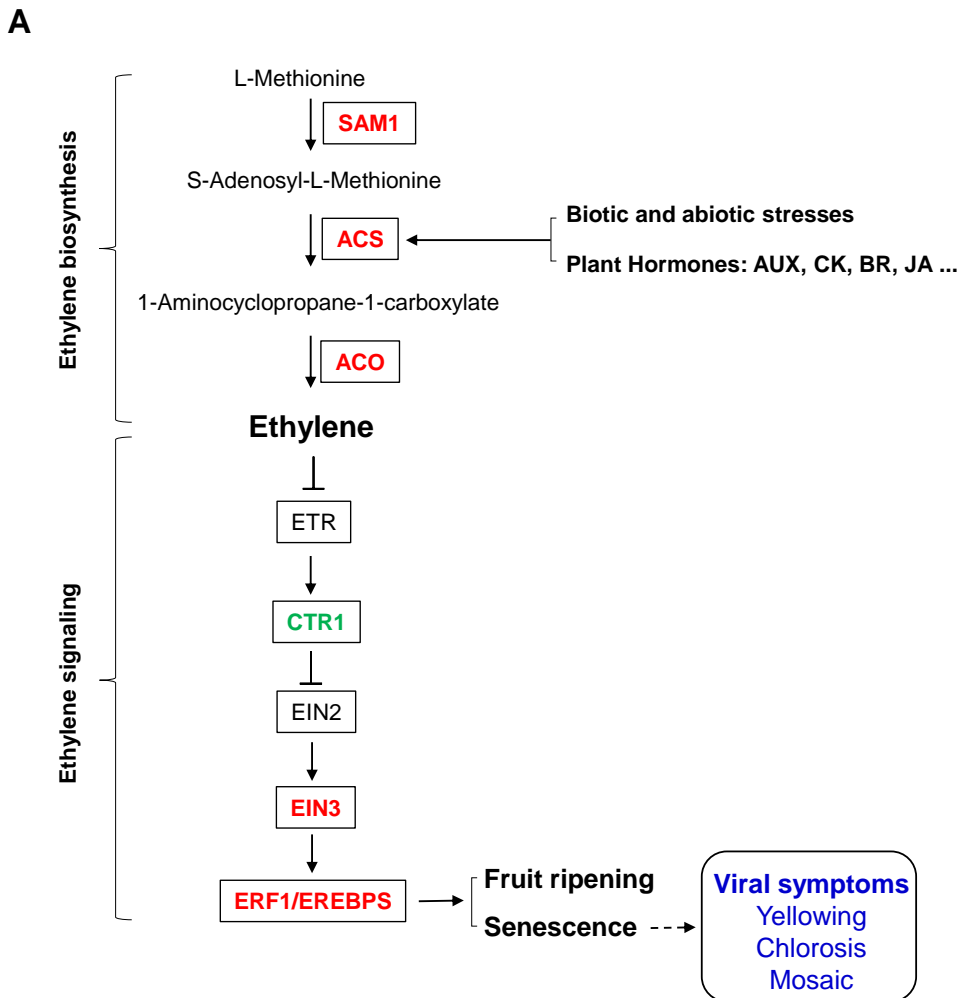
Table 7. DEGs related to Hormone synthesis and signaling in response to infection with CMV

| Gene | Seq. Description | log2 fold change | | | Arabidopsis homolog | TAIR symbol |
|-------------------------|--|------------------|-------|------------|---------------------|-------------|
| | | CMV | BBWV2 | CMV+ BBWV2 | | |
| Auxins | | | | | | |
| CA.PGAV.1.6.scaffold161 | CYT OCHROME P450, FAMILY 71, SUBFAMILY A, POLYPEPTIDE 13 | 1.90 | -0.58 | 1.66 | AT2G30770 | CYP71A13 |
| CA.PGAV.1.6.scaffold161 | Cytochrome P450 83B1-like | 1.62 | -0.15 | 1.85 | AT2G22330 | CYP79B3 |
| CA.PGAV.1.6.scaffold643 | Aldehyde dehydrogenase-like | 1.34 | -0.13 | 1.24 | AT1G44170 | ALDH4 |
| CA.PGAV.1.6.scaffold121 | Probable LRR receptor-like serine/threonine-protein kinase At3g47570 | 1.31 | 0.61 | 1.17 | AT1G20630 | CAT1 |
| CA.PGAV.1.6.scaffold426 | YUCCA 1 | 0.90 | 0.59 | 0.37 | AT4G32540 | YUC1 |
| CA.PGAV.1.6.scaffold133 | CYT OCHROME P450, FAMILY 71, SUBFAMILY A, POLYPEPTIDE 13 | 0.61 | -0.03 | 0.47 | AT2G30770 | CYP71A13 |
| CA.PGAV.1.6.scaffold133 | CYT OCHROME P450, FAMILY 79, SUBFAMILY B, POLYPEPTIDE 2 | 0.61 | -0.03 | 0.47 | AT4G39950 | CYP79B2 |
| CA.PGAV.1.6.scaffold447 | ARABIDOPSIS ALDEHYDE OXIDASE 1 | 0.22 | 0.08 | 0.42 | AT5G20960 | AAO1 |
| CA.PGAV.1.6.scaffold439 | ARABIDOPSIS ALDEHYDE OXIDASE 1 | 0.18 | -0.28 | -0.02 | AT5G20960 | AAO1 |
| CA.PGAV.1.6.scaffold338 | TRYPTOPHAN AMINOTRANSFERASE OF ARABIDOPSIS 1 | 0.08 | 0.30 | 0.23 | AT1G70560 | TAA1 |
| CA.PGAV.1.6.scaffold439 | ARABIDOPSIS ALDEHYDE OXIDASE 1 | 0.00 | -0.17 | -0.95 | AT5G20960 | AAO1 |
| CA.PGAV.1.6.scaffold794 | ARABIDOPSIS ALDEHYDE OXIDASE 1 | -0.03 | 0.11 | -0.09 | AT5G20960 | AAO1 |
| CA.PGAV.1.6.scaffold941 | YUCCA 2 | -0.47 | 0.09 | -1.03 | AT4G13260 | YUC2 |
| CA.PGAV.1.6.scaffold812 | YUCCA 2 | -1.01 | -0.14 | -0.22 | AT4G13260 | YUC2 |
| Cytokins | | | | | | |
| CA.PGAV.1.6.scaffold464 | CYT OCHROME P450, FAMILY 735, SUBFAMILY A, POLYPEPTIDE 2 | 1.56 | 0.97 | 1.50 | AT1G67110 | CYP735A2 |
| CA.PGAV.1.6.scaffold609 | Isopentenyltransferase 5 | 1.38 | 1.03 | 1.03 | AT5G19040 | IPT5 |
| CA.PGAV.1.6.scaffold311 | LONELY GUY 4 | 1.32 | 0.75 | 1.09 | AT3G53450 | LOG4 |
| CA.PGAV.1.6.scaffold158 | CYTOKININ OXIDASE/DEHYDROGENASE 3 | 0.98 | 1.07 | 1.30 | AT5G56970 | CKX3 |
| CA.PGAV.1.6.scaffold123 | CYTOKININ OXIDASE/DEHYDROGENASE 1 | 0.70 | 0.39 | 0.98 | AT2G41510 | CKX1 |
| CA.PGAV.1.6.scaffold292 | Isopentenyltransferase 9, tRNA isopentenyltransferase | 0.40 | -0.38 | 0.40 | AT5G20040 | IPT9 |

| Gene | Seq. Description | log2 fold change | | | Arabidopsis homology | TAIR symbol |
|-------------------------|--|------------------|-------|------------|----------------------|-------------|
| | | CMV | BBWV2 | CMV+ BBWV2 | | |
| Jasmonic acids | | | | | | |
| CA.PGAV.1.6.scaffold500 | JASMONIC ACID CARBOXYL METHYL TRANSFERASE | 2.70 | 1.65 | 4.19 | AT1G19640 | JMT |
| CA.PGAV.1.6.scaffold546 | OPC-8:0 COA LIGASE1 | 0.97 | 0.85 | 0.86 | AT1G20510 | OPCL1 |
| CA.PGAV.1.6.scaffold21 | 4ABNORMAL INFLUORESCENCE MIERSTEM | 0.91 | 1.29 | 1.09 | AT4G29010 | AM1 |
| CA.PGAV.1.6.scaffold21 | 4MULTIFUNCTIONAL PROTEIN 2 | 0.91 | 1.29 | 1.09 | AT3G06860 | MFP2 |
| CA.PGAV.1.6.scaffold140 | DEFECTIVE ANTHRAN DEHISCENCE 1, chloroplastic phospholipase A1 | 0.85 | 0.97 | 1.18 | AT2G44810 | DAD1 |
| CA.PGAV.1.6.scaffold862 | LIPOXYGENASE 3, 13-LOX | 0.64 | 0.14 | 0.56 | AT1G17420 | LOX3 |
| CA.PGAV.1.6.scaffold103 | LIPOXYGENASE 1, 9-LOX, not JA biosynthesis | 0.62 | 0.23 | 1.32 | AT1G55020 | LOX1 |
| CA.PGAV.1.6.scaffold763 | OXOPHYTODIENOATE-REDUCTASE 3 | 0.33 | -0.07 | 0.70 | AT2G06050 | OPR3 |
| CA.PGAV.1.6.scaffold358 | ALLENE OXIDE CYCLASE 3 | -0.64 | -0.61 | -0.61 | AT3G25780 | AOC3 |
| CA.PGAV.1.6.scaffold371 | ALLENE OXIDE SYNTHASE | -1.11 | -0.84 | -0.10 | AT5G42650 | AOS |
| Brassinosteroids | | | | | | |
| CA.PGAV.1.6.scaffold594 | CYCLOARTENOL SYNTHASE 1 | 1.15 | 0.38 | 0.90 | AT2G07050 | CAS1 |
| CA.PGAV.1.6.scaffold594 | CYCLOARTENOL SYNTHASE 1 | 1.11 | 0.30 | 1.36 | AT2G07050 | CAS1 |
| CA.PGAV.1.6.scaffold358 | C90D1 ARATH | 0.92 | 0.39 | 0.84 | AT3G13730 | CYP90D1 |
| CA.PGAV.1.6.scaffold198 | BRASSINOSTEROID-6-OXIDASE 1 | 0.53 | 0.70 | 0.65 | AT5G38970 | Bf6ox1 |
| CA.PGAV.1.6.scaffold497 | BRASSINOSTEROID-6-OXIDASE 2 | 0.50 | 0.62 | -0.09 | AT3G30180 | Bf6ox2 |
| CA.PGAV.1.6.scaffold675 | DWARF 1/CABBAGE 1 | 0.16 | -0.78 | 1.81 | AT3G19820 | DWF1/CBB1 |
| CA.PGAV.1.6.scaffold358 | DWARF 4/CLOWAZONE-RESISTANT1, CYP90B1 | 0.15 | -0.17 | -0.76 | AT3G50660 | DWF4/CLM |
| CA.PGAV.1.6.scaffold284 | DEETIOLATED 2/DWARF 6, steroid-5-alpha-reductase | -0.09 | -0.14 | 0.29 | AT2G38050 | DET2/DWF6 |
| CA.PGAV.1.6.scaffold824 | FACKEL, sterol C-14 reductase | -0.21 | 0.09 | -0.22 | AT3G52940 | FACKEL |
| CA.PGAV.1.6.scaffold824 | FACKEL, sterol C-14 reductase | -0.21 | 0.09 | -0.22 | AT3G52940 | FACKEL |
| CA.PGAV.1.6.scaffold874 | HYDRA1, C-8 sterol isomerase | -0.39 | -0.05 | -0.01 | AT1G20050 | HYD1 |



Figure. 11. Regulation of the genes associated with ethylene biosynthesis upon CMV infection in pepper (A) Ethylene biosynthesis and signaling pathway and key enzymes (B) The DEGs associated with the Ethylene biosynthesis and signaling pathway. Red and Green indicate up- and down-regulation, respectively. S-adenosyl-methionine synthase 1; SAM1, ACC synthase; ACS, ACC oxidase; ACO, constitutive triple response 1; CTR1, ethylene insensitive 3; EIN3, ethylene response factor; ERF1, ethylene-responsive element binding proteins; EREBPs



B

| Gene | Seq. Description | log2 fold change | | | Arabidopsis homolog | TAIR symbol |
|-----------------------------|---|------------------|-------|------------|---------------------|-------------|
| | | CMV | BBWV2 | CMV+ BBWV2 | | |
| CA.PGAV.1.6.scaffold1291.8 | ETHYLENE-RESPONSIVE ELEMENT BINDING FACTOR 13 | 3.59 | 0.73 | 4.11 | AT2G44840 | EREBPIERF13 |
| CA.PGAV.1.6.scaffold1248.38 | ETHYLENE-RESPONSIVE ELEMENT BINDING FACTOR 13 | 1.65 | 0.33 | 1.63 | AT2G44840 | EREBPIERF13 |
| CA.PGAV.1.6.scaffold1784.1 | ACC OXIDASE 3/ETHYLENE FORMING ENZYME | 1.22 | 2.34 | 1.95 | AT1G05010 | ACO4IEFE |
| CA.PGAV.1.6.scaffold1793.14 | ACC OXIDASE 1 | 1.18 | 0.38 | 1.00 | AT2G19590 | ACO1 |
| CA.PGAV.1.6.scaffold1283.5 | ACC OXIDASE 2 | 1.13 | 1.10 | 1.90 | AT1G62380 | ACO2 |
| CA.PGAV.1.6.scaffold1630.30 | ACC SYNTHASE 2 | 1.09 | -0.13 | 0.16 | AT1G01480 | ACS2 |
| CA.PGAV.1.6.scaffold1630.30 | ACC SYNTHASE 10 | 1.09 | -0.13 | 0.16 | AT1G62960 | ACS10 |
| CA.PGAV.1.6.scaffold1075.24 | HOOKLESS 1, Acyl-CoA N-acyltransferases (NAT) superfamily | 0.69 | 0.16 | 0.21 | AT4G37580 | HLS1 |
| CA.PGAV.1.6.scaffold134.44 | ETHYLENE-INSENSITIVE 3 | 0.53 | 0.27 | 0.46 | AT3G20770 | ENS3 |
| CA.PGAV.1.6.scaffold1209.24 | ETHYLENE-RESPONSIVE ELEMENT BINDING FACTOR 13 | 0.50 | 0.48 | 1.24 | AT2G44840 | EREBPIERF13 |
| CA.PGAV.1.6.scaffold1374.18 | S-ADENOSYLMETHIONINE SYNTHETASE 1 | 0.47 | 0.02 | 0.31 | AT1G02500 | SAM1 |
| CA.PGAV.1.6.scaffold1290.20 | ETHYLENE-RESPONSIVE ELEMENT BINDING FACTOR 13 | 0.47 | 0.14 | 0.44 | AT2G44840 | EREBPIERF13 |
| CA.PGAV.1.6.scaffold1363.21 | ETHYLENE-INSENSITIVE 2 | -0.06 | 0.09 | -0.22 | AT5G03280 | EN2 |
| CA.PGAV.1.6.scaffold1247.16 | ETHYLENE-RESPONSIVE ELEMENT BINDING FACTOR 13 | -0.13 | 1.77 | 2.01 | AT2G44840 | EREBPIERF13 |
| CA.PGAV.1.6.scaffold1138.13 | CONSTITUTIVE TRIPLE RESPONSE 1 | -0.24 | 0.11 | -0.92 | AT5G03730 | CTR1 |
| CA.PGAV.1.6.scaffold1129.16 | ENHANCED DISEASE RESISTANCE 1, tomato CTR2 | -0.35 | 0.15 | -0.84 | AT1G08720 | EDR1 |
| CA.PGAV.1.6.scaffold1830.12 | CONSTITUTIVE TRIPLE RESPONSE 1 | -0.56 | -0.27 | -1.05 | AT5G03730 | CTR1 |
| CA.PGAV.1.6.scaffold1532.90 | ETHYLENE-RESPONSIVE ELEMENT BINDING FACTOR 13 | -0.79 | -0.39 | -0.59 | AT2G44840 | EREBPIERF13 |
| CA.PGAV.1.6.scaffold1421.1 | ETHYLENE INSENSITIVE 5/EXORIBONUCLEASE 4 | -0.94 | -0.68 | -1.41 | AT1G54490 | EN5XRN4 |



7. Ethylene production by pepper leaves following CMV infection

To confirm that activation of ethylene pathways is related to accumulation of ethylene in CMV infected leaves, the ethylene production was measured from detached leaves of peppers infected with CMV, BBWV2 and CMV+BBWV2. Ethylene production was enhanced approximately three times more in all virus infected leaves than Healthy controls (Figure. 12). Three replicated experiments revealed that co-infected plants produced much more ethylene than CMV or BBWV2 infected plants.

8. Exogenous ethylene treatment to CMV infected peppers affects symptom development and viral accumulation

To identify the effect of exogenous ethylene treatment to symptom development in CMV infected peppers, we conducted ethylene treatment experiments by using 10mM ethephon (2-chloroethyl phosphonic acid) with different amounts (0ml, 0.5ml, 1ml, 2.5ml). Exogenous ethylene treatment to CMV infected peppers induced severe symptoms including yellowing especially in 2.5ml condition at 3-day after treatment (DAT) (Figure. 13B). In addition, viral accumulation was detected by western blot analysis in extracts of healthy and CMV-infected peppers after ethylene treatment using anti-CP antibody. CMV accumulation was much higher in ethylene treatment peppers than healthy plants (Figure. 13C). The exogenous ethylene-treated plants showed greater susceptibility to CMV infection, displaying more severe disease symptoms and virus accumulation than the CMV-infected plants without ethylene treatment (Figure. 13C).

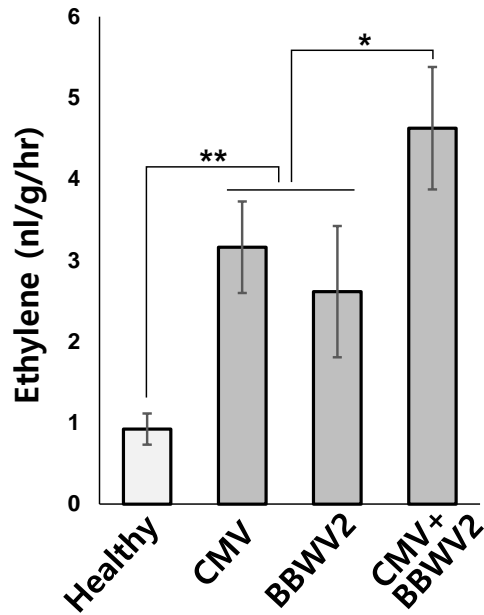
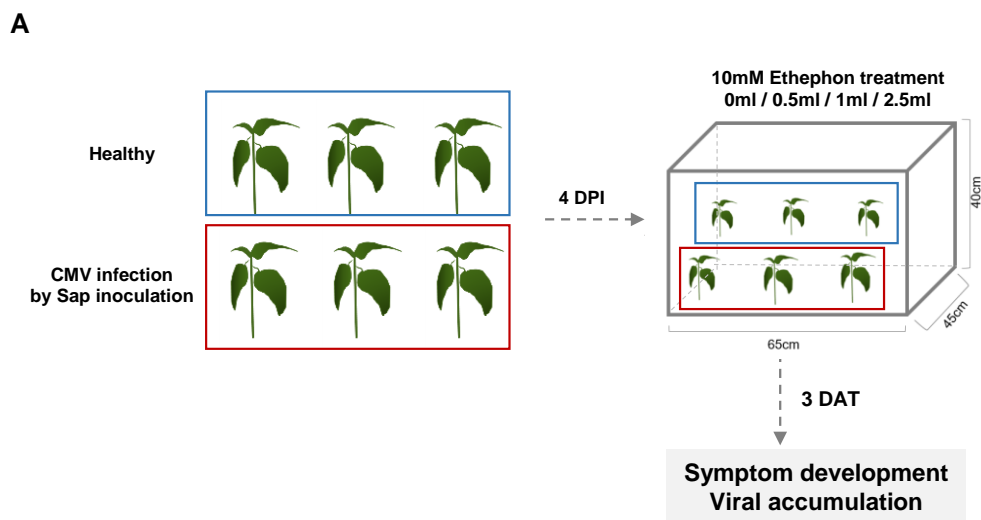


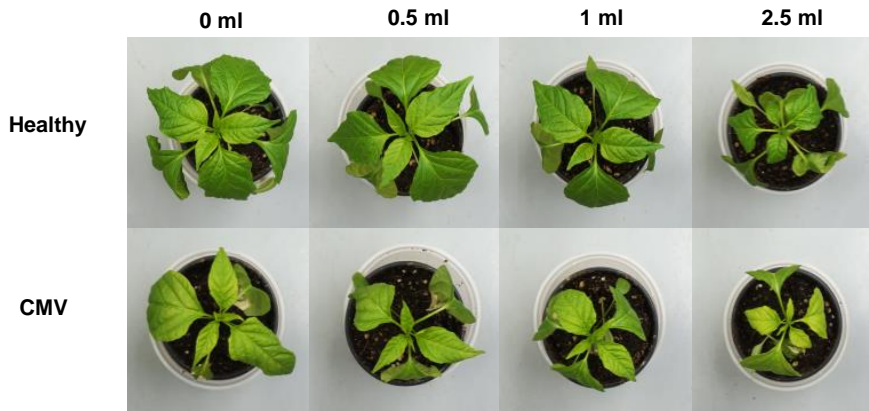
Figure. 12. Ethylene production by detached leaves of peppers infected with CMV, BBWV2 and CMV+BBWV2. Ethylene production rates were measured from symptomatic upper leaves of infected peppers with three air samples and the mean value was calculated. Error bars represent the SEM from three independent experiments. *, $P < 0.05$; **, $P < 0.005$ (determined by Student's t-test).

Figure. 13. Effect of exogenous ethylene on the symptom development and viral accumulation in CMV infected peppers (A) A schematic diagram of the ethylene treatment experiment (B) Symptoms developed at 3 DAT on ethephon treated pepper plants (C) Western blotting analysis of the accumulation CMV coat protein in peppers. The viral accumulation levels were measured by western blotting with the antibody against CMV coat protein. The band density was measured using image J software.

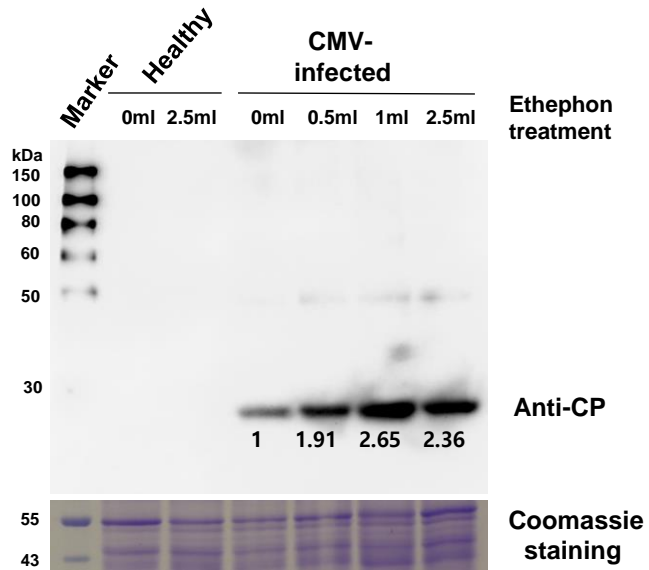


B

10mM Ethephon / 117000 cm³



C



DISCUSSION

Host factors which are essential to viruses could help viral susceptibility by participating in viral life cycles. Identifying the complex molecular interaction between the host plant and virus improves our understanding of the mechanisms related to viral susceptibility and it will help us to find a novel way to control viral diseases. In this study, we utilized proteomic and transcriptomic approaches to identify important genes associated with CMV susceptibility in *N.benthamiana* and pepper plants.

To identify the host factors interacting with CMV proteins by using proteomic approaches, we made FLAG or HA tagging CMV infectious clones (Figure. 1) and performed Co-immunoprecipitation and LC-MS/MS analysis with FLAG:2a which has infectivity in *N.benthamiana* (Figure. 1 and 2A). The Co-IP assay followed by LC-MS/MS analysis has been successfully implemented in virology studies to isolate virus–virus and virus–host multi-protein complexes, allowing the identification of both indirect and direct protein interactions (Lum & Cristea, 2016). We also detected the FLAG:2a proteins in *N.benthamiana* by Western blot using anti-FLAG antibody (Figure. 2C). However, it was reported that CMV could be modified at either or both termini of the 2a protein and at the C-terminus of the 1a protein by insertion of six consecutive histidine residues and remain infectious. These sequences were maintained stably in the viral genome and either displayed no adverse effect or only a moderate effect on the replication and accumulation of the modified virus in tobacco (Gal-On et al., 2000). Thus, unlike His tag sequences, FLAG and HA sequence may have effect on biological properties of CMV1a and MP proteins by affecting their conformation. Charged amino acids of FLAG tags probably induce the conformation change of viral proteins or affect viral genome capacity.

Subcellular localization data showed that 1a:RFP and GFP:2a are localized vacuolar membranes, tonoplasts (Figure. 3). Unlike 1a protein, 2a was also detected in the cytoplasm. It was also reported in tobacco and cucumber plants that the CMV 1a and 2a proteins co-localized predominantly to the tonoplasts. 2a was not observed in the cytoplasm by in situ hybridization. However, Western blotting of fractionated extracts from CMV-infected tissue showed the presence of free, histidine-tagged 2a protein, presumably in the cytoplasm (Cillo et al., 2002). Although subcellular localization of the two proteins was well known, this experiment was meaningful because no data was visualized CMV viral proteins using fluorescent protein as of yet. In addition, we can predict the location of host factors which interact with 1a or 2a around the tonoplast and utilize this information to analyze the Co-IP product.

To investigate the novel cellular interacting partners of CMV 2a, we performed Co-IP and LC-MS/MS analysis. We identified candidate host factors including glyceraldehyde-3-phosphate dehydrogenase-A (GAPDH-A) and eukaryotic translation initiation factor 4A (eIF4A) (Figure. 4C). GAPDHs are ubiquitous enzymes involved in glycolysis and gluconeogenesis, and GAPDH-A is a component of the Calvin-Benson cycle of photosynthetic organisms (Michelet et al., 2013). GAPDH-A and another subunit, GAPDH-B, are both located in the chloroplast in plants and algae (Figge et al., 1999). Recent studies have shown that GAPDH has multiple functions in DNA replication/repair, RNA transport, apoptosis, oxidative stress, membrane fusion, and cytoskeleton assembly (Chaturvedi et al., 2016). In addition, a study identified that GAPDH is an essential host factor for promoting 1a:2a interaction in CMV (Chaturvedi et al., 2016). It is confirmed that there is no CMV accumulation in GAPDH Knockout lines of *A. thaliana* due to the lack of 1a:2a interaction leading to the failure assembly of a functional replicase (Chaturvedi et al., 2016). eIF4A is a DEAD-box ATPase and ATP-dependent RNA helicase. It is well known for unwinding the mRNA

to assist ribosome scanning. eIF4E, eIF4G, eIF4A and other DEAD-box RNA helicases are key translation factors frequently manipulated by viruses (Sanfacon, 2015). There are some evidence that eIF4A assists the translation of Bromovirus and Tombusvirus RNAs (Kovalev et al., 2012; Noueirry et al., 2000). However, no reports about the function of eIF4A in CMV replication has not been made. Interactions between CMV 2a and the candidate proteins remain to be further verified.

Symptoms are the result of interactions between the plant and the virus. The interactions cause distinct symptoms to the plant for each virus. To reveal the host factors which are highly regulated by CMV infection, we analyzed the significant differences in the regulation of gene expression among CMV, BBWV2 and co-infected peppers by using transcriptomic approach. The results showed that a total of 393 DEGs, 214 DEGs and 801 DEGs were significantly regulated by CMV, BBWV2 and CMV+BBWV2. A total of 129 genes are commonly up-regulated upon CMV, BBWV2 and co-infection. Only 2 genes are commonly up-regulated by CMV and BBWV2 (Figure. 6A and 6B). These findings indicate that CMV and BBWV2 are involved in the different metabolic, physiological and developmental processes in peppers. Since a lot of genes were co-regulated by CMV and CMV+BBWV2, there may be a synergistic relationship in the regulation of cellular processes between CMV and BBWV2 (Figure. 6B). According to the top 20 DEGs in CMV infected peppers (Table. 3), various stress-related and hormone-related genes were transcriptionally up-regulated. On the other hand, cell-cycle and plant volatiles-related genes were mainly down-regulated upon CMV infection.

Comparative analysis of DEGs using GO terms showed that up-regulated DEGs in CMV infected peppers were associated with responses to stimulus and hormones (Figure. 8). In addition, down-regulated DEGs were significantly related to cell cycle and cell division (Figure. 9). We found that

DEGs associated with cell division such as inactive receptor kinase (PUTATIVE KINASE), cyclin-D3 (CYCD3), cyclin-A1 (CYCA1), cyclin-A2 (CYCA2), condensin complex subunit 1 (CAP-D2), fatty acyl-coA reductase 3-like isoform X1 (CER4) were repressed during CMV infection (Figure. 10). Cell cycle regulation is important for plant growth and development. Cyclin proteins and cyclin-dependent kinases (CDKs) are key regulators of cell division (Morgan, 1997). D-type cyclins including CYCD3 regulate the G1-to-S transition and A-type cyclins control the S-to-M phase transition (Inzé & Veylder, 2006). Some reports demonstrated that the expression of D-type cyclin genes is modulated by plant hormones such as cytokinins, auxins, brassinosteroids and gibberellins (Hu et al., 2000; Richard et al., 2002; Sauter et al., 1995). Thus, it is possibly that down-regulation of the genes related to the cell cycle is related to stunting and leaf size reduction induced by CMV. However, the molecular mechanisms between hormones and cell cycle-related genes should be further investigated to confirm their functions in plant growth and development.

As a result of KEGG analysis using arabidopsis orthologs, we found that plant hormone signal transduction, Cysteine and methionine metabolism and biosynthesis of secondary metabolites were enriched (Table. 6). Interestingly, DEGs were mainly associated with related to ethylene synthesis and signaling. Ethylene is identified as a plant hormone known to regulate numerous processes in fruit ripening, plant growth, development, and response to biotic and abiotic stresses (Hao. et al., 2017). Our data showed that the key enzymes of ethylene biosynthesis such as SAM synthetase (SAM1), ACC synthetase (ACS) and ACC oxidase (ACO) were up-regulated in CMV infection (Figure. 11). It is reported that ethylene biosynthesis is regulated at the level of ACC synthetase (ACS). In addition, ACS induction and activation are responsive to environmental factors that trigger ethylene accumulation (Dubois et al., 2018). CONSTITUTIVE TRIPLE RESPONSE1 (CTR1) which is a negative

regulator of a Mitogen-activated protein kinase (MAPK) cascade was down-regulated upon CMV infection (Dugardeyn. et al., 2007). Other ethylene signaling pathway associated DEGs such as ETHYLENE INSENSITIVE 3 (EIN3) were activated to promote ethylene responses (Figure. 11).

We suggest that modulating hormone-related host genes by CMV infection might be correlated with CMV symptoms. For example, ethylene production has been found to be associated with the development of local necrotic and chlorotic lesions, epinasty, retardation of epicotyl growth, and hypocotyl elongation (Nakagaki et al., 1970; Pritchard & Ross, 1975). It has been reported in cucumber that ethylene is involved in the development of CMV-induced chlorotic lesions and in tobacco that ethylene production is stimulated by CMV infection (ShlomoMarc. & DavidLevy., 1979). In this study, we confirmed the increase in ethylene production upon CMV infection and in symptom severity when the pepper plants were treated with high concentration of ethylene (Figure. 13 and 14). In addition, the higher the ethylene treatment concentration, the more CMV replications occurred (Figure. 14). The results indicate that ethylene has specific roles in CMV infected peppers related to CMV replication and symptom development. Some studies suggest that CMV infection positively influence ethylene biosynthesis through the regulation of ACS and ACC oxidase activities (Chaudhry. et al., 1998; ShlomoMarc. & DavidLevy., 1979), whereas how ethylene affects the CMV replication remains unclear. Several studies have found that viruses can alter plant defense signaling and modify the volatiles released from the plant in ways that attract or vector insects (Guo et al., 2019; Mauck et al., 2010, 2014; Wu et al., 2017). Ethylene is one of the plant volatile organic compounds (VOCs) which have multiple functions including modification of intercellular transport (Dorokhov. et al., 2014). Intercellular transport is an essential process for viruses to replicate their genomes inside plant cells. It is possible that the increase in ethylene might be a strategy to increase vector transmission by modulating

gene expressions. Further research into the relation between ethylene and vector attraction will be needed.

In this research, host factors that are considered as related to CMV infection were analyzed through proteomic and transcriptomic approaches. Controlling these factors will be able to be one of the methods that can keep crop production as they can prevent either infection itself or symptoms from appearing despite infection. Our approaches can provide new insights into enhancing plant immunity against viral diseases.

REFERENCES

Carbonell A., García J. A., Simón-Mateo C., Hernández C. (2016) Plant Virus RNA Replication. *eLS. John Wiley & Sons.*

Chaturvedi S., Seo J. K., Rao A. L. (2016) Functionality of host proteins in Cucumber mosaic virus replication: GAPDH is obligatory to promote interaction between replication-associated proteins. *Virology*. **494**, 47-55.

Chaudhry. Z., Yoshioka. T., Satoh. S., Hase. S., Ehara. Y. (1998) Stimulated ethylene production in tobacco (*Nicotiana tabacum* L. cv. Ky 57) leaves infected systemically with cucumber mosaic virus yellow strain. **131**, 123-130.

Cillo F., Roberts I. M., Palukaitis P. (2002) In situ localization and tissue distribution of the replication-associated proteins of Cucumber mosaic virus in tobacco and cucumber. *J Virol*. **76**, 10654-10664.

Culver J. N., Padmanabhan M. S. (2007) Virus-induced disease: altering host physiology one interaction at a time. *Annu Rev Phytopathol*. **45**, 221-243.

DAC P., P H. (2002) Plant Resistance and Strategies for Breeding Resistant Varieties. *Plant Protection Science*. **38**, 9-13.

Dorokhov. Y. L., Komarova. T. V., Sheshukova E. V. (2014) Volatile organic compounds and plant virus–host interaction. *Plant Virus-Host Interaction: Molecular Approaches and Viral Evolution*. 241-262.

Dubois M., Van den Broeck L., Inze D. (2018) The Pivotal Role of Ethylene in Plant Growth. *Trends Plant Sci.* **23**, 311-323.

Dugardeyn. J., Vandenbussche. F., Straeten. D. V. D. (2007) To grow or not to grow: what can we learn on ethylene-gibberellin cross-talk by *in silico* gene expression analysis? *Journal of Experimental Botany.* **59**, 1-16.

Ferrer R. M., Ferriol I., Moreno P., Guerri J., Rubio L. (2011) Genetic variation and evolutionary analysis of broad bean wilt virus 2. *Arch Virol.* **156**, 1445-1450.

Figge R. M., Schubert M., Brinkmann H., Cerff R. (1999) Glyceraldehyde-3-phosphate dehydrogenase gene diversity in eubacteria and eukaryotes: evidence for intra- and inter-kingdom gene transfer. *Mol Biol Evol.* **16**, 429-440.

Gal-On A., Canto T., Palukaitis P. (2000) Characterisation of genetically modified cucumber mosaic virus expressing histidine-tagged 1a and 2a proteins. *Arch Virol.* **145**, 37-50.

Gallitelli D. (2000) The ecology of Cucumber mosaic virus and sustainable agriculture. *Virus Res.* **71**, 9-21.

Guo H., Gu L., Liu F., Chen F., Ge F., Sun Y. (2019) Aphid-borne Viral Spread Is Enhanced by Virus-induced Accumulation of Plant Reactive Oxygen Species. *Plant Physiol.* **179**, 143-155.

Hao. D., Sun. X., Ma. B., Zhang. J.-S., Guo. H. (2017) 6 - Ethylene. *Hormone Metabolism and Signaling in Plants.* 203-241.

Hashimoto M., Neriya Y., Yamaji Y., Namba S. (2016) Recessive Resistance to Plant Viruses: Potential Resistance Genes Beyond Translation Initiation Factors. *Front Microbiol.* **7**, 1695.

Hu Y., Bao F., Li J. (2000) Promotive effect of brassinosteroids on cell division involves a distinct CycD3-induction pathway in Arabidopsis. *Plant J.* **24**, 693-701.

Huang da W., Sherman B. T., Lempicki R. A. (2009) Systematic and integrative analysis of large gene lists using DAVID bioinformatics resources. *Nat Protoc.* **4**, 44-57.

Inzé D., Veylder L. D. (2006) Cell Cycle Regulation in Plant Development. *Annual Review of Genetics.* **40**, 77-105.

Kang B. C., Yeam I., Jahn M. M. (2005) Genetics of plant virus resistance. *Annu Rev Phytopathol.* **43**, 581-621.

Kim M. J., Kim H. R., Paek K. H. (2006) Arabidopsis tonoplast proteins TIP1 and TIP2 interact with the cucumber mosaic virus 1a replication protein. *J Gen Virol.* **87**, 3425-3431.

Kim S. H., Palukaitis P., Park Y. I. (2002) Phosphorylation of cucumber mosaic virus RNA polymerase 2a protein inhibits formation of replicase complex. *EMBO J.* **21**, 2292-2300.

Kong L. J., Orozco B. M., Roe J. L., Nagar S., Ou S., Feiler H. S., Durfee T., Miller A. B., Grussem W., Robertson D., Hanley-Bowdoin L. (2000) A geminivirus replication protein interacts with the retinoblastoma protein

through a novel domain to determine symptoms and tissue specificity of infection in plants. *EMBO J.* **19**, 3485-3495.

Kovalev N., Pogany J., Nagy P. D. (2012) A Co-Opted DEAD-Box RNA helicase enhances tombusvirus plus-strand synthesis. *PLoS Pathog.* **8**, e1002537.

Kwon S.-J., Cho I.-S., Yoon J.-Y., Chung B.-N. (2018) Incidence and Occurrence Pattern of Viruses on Peppers Growing in Fields in Korea. *Res. Plant Dis.* **24**, 66-74.

Legg J. P., Shirima R., Tajebe L. S., Guastella D., Boniface S., Jeremiah S., Nsami E., Chikoti P., Rapisarda C. (2014) Biology and management of Bemisia whitefly vectors of cassava virus pandemics in Africa. *Pest Manag Sci.* **70**, 1446-1453.

Loebenstein G., Katis N. (2014) Control of plant virus diseases seed-propagated crops. Preface. *Adv Virus Res.* **90**, xi.

Lum K. K., Cristea I. M. (2016) Proteomic approaches to uncovering virus-host protein interactions during the progression of viral infection. *Expert Rev Proteomics.* **13**, 325-340.

Mauck K. E., De Moraes C. M., Mescher M. C. (2010) Deceptive chemical signals induced by a plant virus attract insect vectors to inferior hosts. *Proc Natl Acad Sci U S A.* **107**, 3600-3605.

Mauck K. E., De Moraes C. M., Mescher M. C. (2014) Biochemical and physiological mechanisms underlying effects of Cucumber mosaic virus on

host-plant traits that mediate transmission by aphid vectors. *Plant Cell Environ.* **37**, 1427-1439.

Mazier M., Flamain F., Nicolai M., Sarnette V., Caranta C. (2011) Knock-down of both eIF4E1 and eIF4E2 genes confers broad-spectrum resistance against potyviruses in tomato. *PLoS One.* **6**, e29595.

Michelet L., Zaffagnini M., Morisse S., Sparla F., Perez-Perez M. E., Francia F., Danon A., Marchand C. H., Fermani S., Trost P., Lemaire S. D. (2013) Redox regulation of the Calvin-Benson cycle: something old, something new. *Front Plant Sci.* **4**, 470.

Moffett P. (2009) Mechanisms of recognition in dominant R gene mediated resistance. *Adv Virus Res.* **75**, 1-33.

Morgan D. O. (1997) Cyclin-dependent kinases: engines, clocks, and microprocessors. *Annu Rev Cell Dev Biol.* **13**, 261-291.

Nagy P. D., Pogany J. (2011) The dependence of viral RNA replication on co-opted host factors. *Nat Rev Microbiol.* **10**, 137-149.

Nakagaki Y., Hirai T., Stahmann M. A. (1970) Ethylene production by detached leaves infected with tobacco mosaic virus. *Virology.* **40**, 1-9.

Noueiry A. O., Chen J., Ahlquist P. (2000) A mutant allele of essential, general translation initiation factor DED1 selectively inhibits translation of a viral mRNA. *Proc Natl Acad Sci U S A.* **97**, 12985-12990.

Pallas V., Antonio J. (2011) How do plant viruses induce disease? Interactions and interference with host components. *Journal of General Virology*. **92**, 2691–2705.

Palukaitis P., Garcia-Arenal F. (2003) Cucumoviruses. *Adv Virus Res*. **62**, 241-323.

Pritchard D. W., Ross A. F. (1975) The relationship of ethylene to formation of tobacco mosaic virus lesions in hypersensitive responding tobacco leaves with and without induced resistance. *Virology*. **64**, 295-307.

Richard C., Lescot M., Inzé D., De Veylder L. (2002) Effect of auxin, cytokinin, and sucrose on cell cycle gene expression in *Arabidopsis thaliana* cell suspension cultures. *Plant Cell, Tissue and Organ Culture*. **69**, 167-176.

Robaglia C., Caranta C. (2006) Translation initiation factors: a weak link in plant RNA virus infection. *Trends Plant Sci*. **11**, 40-45.

Sanfacon H. (2015) Plant Translation Factors and Virus Resistance. *Viruses*. **7**, 3392-3419.

Sauter M., Mekhedov S. L., Kende H. (1995) Gibberellin promotes histone H1 kinase activity and the expression of *cdc2* and *cyclin* genes during the induction of rapid growth in deepwater rice internodes. *Plant J*. **7**, 623-632.

Seo J. K., Kim M. K., Kwak H. R., Choi H. S., Nam M., Choe J., Choi B., Han S. J., Kang J. H., Jung C. (2018) Molecular dissection of distinct symptoms induced by tomato chlorosis virus and tomato yellow leaf curl virus based on comparative transcriptome analysis. *Virology*. **516**, 1-20.

Seo J. K., Kwon S. J., Choi H. S., Kim K. H. (2009) Evidence for alternate states of Cucumber mosaic virus replicase assembly in positive- and negative-strand RNA synthesis. *Virology*. **383**, 248-260.

ShlomoMarc., DavidLevy. (1979) Involvement of ethylene in the development of cucumber mosaic virus-induced chlorotic lesions in cucumber cotyledonst. *Physiological Plant Pathology*. **14**, 235-244.

Supek F., Bosnjak M., Skunca N., Smuc T. (2011) REVIGO summarizes and visualizes long lists of gene ontology terms. *PLoS One*. **6**, e21800.

Truniger V., Aranda M. A. (2009) Recessive resistance to plant viruses. *Adv. Virus Res.* **75**, 119-159.

Wang A. (2015) Dissecting the molecular network of virus-plant interactions: the complex roles of host factors. *Annu Rev Phytopathol.* **53**, 45-66.

Wang A. (2018) Virus and Host Plant Interactions. *eLS. John Wiley & Sons.*

Wang K. L., Li H., Ecker J. R. (2002) Ethylene biosynthesis and signaling networks. *Plant Cell*. **14 Suppl**, S131-151.

Whitham S. A., Quan S., Chang H. S., Cooper B., Estes B., Zhu T., Wang X., Hou Y. M. (2003) Diverse RNA viruses elicit the expression of common sets of genes in susceptible *Arabidopsis thaliana* plants. *Plant J.* **33**, 271-283.

Wu D., Qi T., Li W. X., Tian H., Gao H., Wang J., Ge J., Yao R., Ren C., Wang X. B., Liu Y., Kang L., Ding S. W., Xie D. (2017) Viral effector protein manipulates host hormone signaling to attract insect vectors. *Cell Res.* **27**, 402-415.

Zaidi S. S., Tashkandi M., Mansoor S., Mahfouz M. M. (2016) Engineering Plant Immunity: Using CRISPR/Cas9 to Generate Virus Resistance. *Front Plant Sci.* **7**, 1673.

ABSTRACT IN KOREAN

단백체 및 전사체 분석을 통한 오이모자이크 바이러스 감수성 관련 기주 인자 구명

한수정

초록

식물 바이러스병은 작물 생산량 손실을 일으키는 주요 병원균 중 하나로, 돌연변이 발생이 빈번하고 치료 약제가 개발되어 있지 않아 방제가 매우 어렵다. 이러한 바이러스병을 방제하기 위한 가장 효과적인 방법은 저항성 품종을 재배하는 것이며, 바이러스 저항성 품종을 개발하기 위해서는 바이러스와 기주 식물 간의 다양한 유전자적 상호작용에 대한 정확한 이해가 필요하다. 식물의 열성 저항성은 병원체가 살아가는데 필요한 식물 유전자가 결핍되었을 때 획득되는데, 우성 저항성에 비해 넓은 범위의 저항성을 발현하고 돌연변이 출현에 쉽게 저항성이 상실되지 않는 특성을 보인다. 본 연구에서는 열성 저항성을 유도할 수 있는 유전적 자원을 확보하기 위해 우리 나라 고추에 심각한 피해를 입히는 것으로 잘 알려진 오이모자이크 바이러스 (CMV)와

상호작용하는 기주 유전자를 밝히고자 했다. 우리는 CMV 의 기주 유전자를 구명하기 위하여 단백질 및 전사체 분석을 실시하였다.

단백체 분석에서는 CMV 감염성 클론에 FLAG 과 HA tag 을 붙여 CO-IP 와 LC-MS/MS 를 통해 후보 기주 인자를 찾으려고 했으며, 접종 후 *N.benthamiana* 에서 감염성이 유지된 FLAG-2a 클론을 이용하여 Co-IP 와 LC-MS/MS 분석을 통해 다양한 후보 유전자를 찾아냈다. 또한, 형광 단백질을 재조합한 1a 와 2a 단백질의 세포 내 localization 을 관찰하여 후보 유전자들의 작용 위치를 예상할 수 있었다. 우리는 또한 고추에서 CMV 증상 발현 과정 동안 조절되는 기주 유전자를 밝히기 위해 RNA 시퀀싱 분석을 이용하였다. GO term 과 KEGG pathway 를 이용한 DEG 의 비교 분석 결과 주로 스트레스 반응 관련 유전자들과 호르몬 관련 유전자들이 CMV 의 감염으로 주로 조절되는 것을 확인하였다. 특히, 호르몬 중에서 특히 에틸렌 합성과 신호전달 관련 DEG 들이 CMV 감염에 의해 상향 조절되었다. 실제 GC 분석 결과, CMV 감염 시 에틸렌 생산이 증가하였으며, 외부에서 에틸렌을 처리했을 때 처리 농도의 증가에 따라 증상이 심해지고 CMV 축적량도 증가하는 것을 확인하였다. 추가적으로, 세포 분열 조절과 관련된 유전자들은 주로 하향 조절되는 것이 확인되었다. CMV 감염 시 호르몬과 세포 주기 관련 기주 유전자들이 조절되는 것은 CMV 의 대표적인 mosaic, chlorosis, stunting 증상과 관련이 있을 것으로 보인다. 본 연구 결과는 오이모자이크바이러스의 증식에 필수적인 다양한 기주 인자를 밝혀내기 위한 중요한 기초 자료가 될 것이며,

이를 통해 열성 저항성 작물 개발을 위한 유용한 유전적 자원이 확보될 수 있을 것으로 사려된다.

주요어: 열성 저항성, 기주-바이러스 상호작용, 오이모자이크 바이러스, 기주 인자, 감수성 유전자

감사의 글

많은 분들의 도움으로 이 논문을 완성할 수 있었기에 감사의 인사를 전합니다. 먼저 공부할 수 있도록 기회를 주신 서장균 교수님께 깊은 감사의 말씀을 드립니다. 짧은 석사 과정 동안이었지만 저에게 다양한 경험을 할 수 있는 기회를 주시고 제가 스스로 해낼 수 있도록 늘 묵묵히 지켜봐 주셔서 감사합니다. 바쁘신 가운데 연구에 대한 조언과 격려를 아끼지 않으셨던 김주곤 교수님, 강진호 교수님, 정춘균 교수님께도 고개 숙여 감사의 인사를 드리고 싶습니다.

평창에서 가장 오랜 시간을 함께 보낸 연구실 식구들도 고맙습니다. 항상 따뜻한 말과 행동으로 저를 돌봐준 보람언니, 최고의 고민 해결사 시원이, 재미없는 이야기도 다 들어주고 받아주는 다정한 경재, 늘 세심한 배려로 감동을 주는 명휘. 바쁘다는 핑계로 많이 챙겨주지 못한 것 같아 미안했고 늘 신경 써주고 이해해줘서 고맙습니다.

사랑하는 누리, 당당하고 멋진 소윤, 배려 깊은 서원, 밝은 웃음을 가진 주연, 귀여운 재인, 멋쟁이 원기, 싹싹한 지민, 개구쟁이 대현, 모범생 성민, 발랄한 막내 문주에게도 고맙고 덕분에 평창 생활이 더욱 즐거웠습니다. 나의 영원한 룸메 미향, 당찬 유안이, 지금은 다른 자리에서 열심히 지내고 있는 나래, 희진, 주희, 성환에게도 고맙다는 인사를 전하고 싶습니다.

마지막으로 언제나 뒤에서 든든한 버팀목이 되어주시는 부모님, 언니, 미녀 동생도 고맙습니다. 힘들고 지칠 때마다 옆에서 응원을 아끼지 않았던 우리 이쁜 미션이들, 지은이들, 세은이, 아름이, 소라, 용선, 정현언니도 고맙습니다. 앞으로 더 좋은 모습으로 보답하겠습니다.